tissue protection through an erythropoietin and common β-subunit heteroreceptor. Proc Natl Acad Sci USA 101:14907–14912.
6. Guimond SE, Turnbull JE (2005). Heparan sulphate-growth factor interactions in development and growth. Trends. Glycosci. Glycotechnol. 17: 241–253.
7. Pandya NM, Dhalla NS, Santani DD. (2006). Angiogenesis–a new target for future therapy. Vascul Pharmacol 44:265–274.
8. Los M, Roodhart JM, Voest EE. (2007). Target practice: lessons from phase III trials with bevacizumab and vatalanib in the treatment of advanced colorectal cancer. Oncologist 12:443–450.
9. Motzer RJ, Escudier B, Oudard S, Hutson TE, Porta C, Bracarda S, Grünwald V, Thompson JA, Figlin RA, Hollaender N, Kay A, Ravaud A; RECORD-1 Study Group. (2010). Phase 3 trial of everolimus for metastatic renal cell carcinoma: final results and analysis of prognostic factors. Cancer 116:4256–4265.
10. O'Reilly MS, Holmgren L, Shing Y, Chen C, Rosenthal RA, Moses M, Lane WS, Cao Y, Sage EH, Folkman J. (1994). Angiostatin: a novel angiogenesis inhibitor that mediates the suppression of metastases by a Lewis lung carcinoma. Cell 79:315–328.
11. Folkman J. (2006). Antiangiogenesis in cancer therapy–endostatin and its mechanisms of action. Exp Cell Res 312:594–607.
12. Ding YH, Javaherian K, Lo KM, Chopra R, Boehm T, Lanciotti J, Harris BA, Li Y, Shapiro R, Hohenester E, Timpl R, Folkman J, Wiley DC. (1998). Zinc-dependent dimers observed in crystals of human endostatin. Proc Natl Acad Sci USA 95:10443–10448.
13. Karumanchi SA, Jha V, Ramchandran R, Karihaloo A, Tsiokas L, Chan B, Dhanabal M, Hanai JI, Venkataraman G, Shriver Z, Keiser N, Kalluri R, Zeng H, Mukhopadhyay D, Chen RL, Lander AD, Hagihara K, Yamaguchi Y, Sasisekharan R, Cantley L, Sukhatme VP. (2001). Cell surface glypicans are low-affinity endostatin receptors. Mol Cell 7:811–822.
14. Wang J, Sun Y, Liu Y, Yu Q, Zhang Y, Li K, Zhu Y, Zhou Q, Hou M, Guan Z, Li W, Zhuang W, Wang D, Liang H, Qin F, Lu H, Liu X, Sun H, Zhang Y, Wang J, Luo S, Yang R, Tu Y, Wang X, Song S, Zhou J, You L, Wang J, Yao C. (2005). [Results of randomized, multicenter, double-blind phase III trial of rh-endostatin (YH-16) in treatment of advanced non-small cell lung cancer patients.]. Zhongguo Fei Ai Za Zhi 8:283–290.
15. Fischer C, Mazzone M, Jonckx B, Carmeliet P. (2008). FLT1 and its ligands VEGFB and PlGF: drug targets for anti-angiogenic therapy? Nat Rev Cancer 8:942–956.
16. Loges S, Schmidt T, Carmeliet P. (2009). "Antimyeloangiogenic" therapy for cancer by inhibiting PlGF. Clin Cancer Res 15:3648–3653.
17. De Falco S, Gigante B, Persico MG. (2002). Structure and function of placental growth factor. Trends Cardiovasc Med 12:241–246.
18. Nagy JA, Dvorak AM, Dvorak HF. (2003). VEGF-A(164/165) and PlGF: roles in angiogenesis and arteriogenesis. Trends Cardiovasc Med 13:169–175.
19. Miyazaki Y, Kuriyama K, Higuchi M, Tsushima H, Sohda H, Imai N, Saito M, Kondo T, Tomonaga M. (1997). Establishment and characterization of a new erythropoietin-dependent acute myeloid leukemia cell line, AS-E2. Leukemia 11:1941–1949.
20. Lee GY, Jung WW, Kang CS, Bang IS. (2006). Expression and characterization of human vascular endothelial growth factor (VEGF165) in insect cells. Protein Expr Purif 46:503–509.
21. Ozawa T, Toba K, Kato K, Minagawa S, Saigawa T, Hanawa H, Makiyama Y, Moriyama M, Honma K, Isoda M, Hasegawa G, Naito M, Takahashi M, Aizawa Y. (2006). Erythroid cells play essential roles in angiogenesis by bone marrow cell implantation. J Mol Cell Cardiol 40:629–638.
22. Middleton SA, Barbone FP, Johnson DL, Thurmond RL, You Y, McMahon FJ, Jin R, Livnah O, Tullai J, Farrell FX, Goldsmith MA, Wilson IA, Jolliffe LK. (1999). Shared and unique determinants of the erythropoietin (EPO) receptor are important for binding EPO and EPO mimetic peptide. J Biol Chem 274:14163–14169.
23. Fukuda MN, Sasaki H, Lopez L, Fukuda M. (1989). Survival of recombinant erythropoietin in the circulation: the role of carbohydrates. Blood 73:84–89.
24. Vanrenterghem Y, Bárány P, Mann JF, Kerr PG, Wilson J, Baker NF, Gray SJ; European/Australian NESP 970200 Study Group. (2002). Randomized trial of darbepoetin alfa for treatment of renal anemia at a reduced dose frequency compared with rHuEPO in dialysis patients. Kidney Int 62:2167–2175.
25. Macdougall IC. (2005). CERA (Continuous Erythropoietin Receptor Activator): a new erythropoiesis-stimulating agent for the treatment of anemia. Curr Hematol Rep 4:436–440.
26. Yamaguchi N, Anand-Apte B, Lee M, Sasaki T, Fukai N, Shapiro R, Que I, Lowik C, Timpl R, Olsen BR. (1999). Endostatin inhibits VEGF-induced endothelial cell migration and tumor growth independently of zinc binding. EMBO J 18:4414–4423.
27. Glaspy JA. (2009). Erythropoietin in cancer patients. Annu Rev Med 60:181–192.
28. Rizzo JD, Brouwers M, Hurley P, Seidenfeld J, Arcasoy MO, Spivak JL, Bennett CL, Bohlius J, Evanchuk D, Goode MJ, Jakubowski AA, Regan DH, Somerfield MR; American Society of Hematology and the American Society of Clinical Oncology Practice Guideline Update Committee. (2010). American Society of Hematology/American Society of Clinical Oncology clinical practice guideline update on the use of epoetin and darbepoetin in adult patients with cancer. Blood 116:4045–4059.
29. Parsa CJ, Matsumoto A, Kim J, Riel RU, Pascal LS, Walton GB, Thompson RB, Petrofski JA, Annex BH, Stamler JS, Koch WJ. (2003). A novel protective effect of erythropoietin in the infarcted heart. J Clin Invest 112:999–1007.
30. Hirata A, Minamino T, Asanuma H, Fujita M, Wakeno M, Myoishi M, Tsukamoto O, Okada K, Koyama H, Komamura K, Takashima S, Shinozaki Y, Mori H, Shiraga M, Kitakaze M, Hori M. (2006). Erythropoietin enhances neovascularization of ischemic myocardium and improves left ventricular dysfunction after myocardial infarction in dogs. J Am Coll Cardiol 48:176–184.
31. Mitsuma W, Ito M, Kodama M, Fuse K, Okamura K, Minagawa S, Kato K, Hanawa H, Toba K, Nakazawa M, Aizawa Y. (2006). Cardioprotective effects of recombinant human erythropoietin in rats with experimental autoimmune myocarditis. Biochem Biophys Res Commun 344:987–994.
32. Ozawa T, Toba K, Suzuki H, Kato K, Iso Y, Akutsu Y, Kobayashi Y, Takeyama Y, Kobayashi N, Yoshimura N, Akazawa K, Aizawa Y; EPO/AMI-I Pilot Study Researchers. (2010). Single-dose intravenous administration of recombinant human erythropoietin is a promising treatment for patients with acute myocardial infarction – randomized controlled pilot trial of EPO/AMI-1 study -. Circ J 74:1415–1423.
33. Toba K, Kato K, Ozawa T, Aizawa Y. (2011). [Clinical study from Japan and its reflections: evaluation of the prospective observation of erythropoietin-administration for the treatment of acute myocardial infarction (EPO/AMI-1) study]. Nippon Naika Gakkai Zasshi 100:2008–2014.
34. Voors AA, Belonje AM, Zijlstra F, Hillege HL, Anker SD, Slart RH, Tio RA, van 't Hof A, Jukema JW, Peels HO, Henriques JP, Ten Berg JM, Vos J, van Gilst WH, van Veldhuisen DJ; HEBE III Investigators. (2010). A single dose of erythropoietin in ST-elevation myocardial infarction. Eur Heart J 31:2593–2600.
35. Ott I, Schulz S, Mehilli J, Fichtner S, Hadamitzky M, Hoppe K, Ibrahim T, Martinoff S, Massberg S, Laugwitz KL, Dirschinger J, Schwaiger M, Kastrati A, Schmig A; REVIVAL-3 Study Investigators. (2010). Erythropoietin in patients with acute ST-segment elevation myocardial infarction undergoing primary percutaneous coronary intervention: a randomized, double-blind trial. Circ Cardiovasc Interv 3:408–413.
36. Vaziri ND. (2009). Thrombocytosis in EPO-treated dialysis patients may be mediated by EPO rather than iron deficiency. Am J Kidney Dis 53:733–736.
37. Baker JE, Kozik D, Hsu AK, Fu X, Tweddell JS, Gross GJ. (2007). Darbepoetin alfa protects the rat heart against infarction: dose-response, phase of action, and mechanisms. J Cardiovasc Pharmacol 49:337–345.
38. Ogino A, Takemura G, Kawasaki M, Tsujimoto A, Kanamori H, Li L, Goto K, Maruyama R, Kawamura I, Takeyama T, Kawaguchi T, Watanabe T, Moriguchi Y, Saito H, Fujiwara T, Fujiwara H, Minatoguchi S. (2010). Erythropoietin receptor signaling mitigates renal dysfunction-associated heart failure by mechanisms unrelated to relief of anemia. J Am Coll Cardiol 56:1949–1958.

Clinical and Experimental Hypertension, 2012; Early Online: 1–7

ISSN 1064-1963 print/1525-6006 online
DOI: 10.3109/10641963.2012.681728

informa
healthcare

Erythropoietin, but Not Asialoerythropoietin or Carbamyl-Erythropoietin, Attenuates Monocrotaline-Induced Pulmonary Hypertension in Rats

Noboru Ikarashi,[1] Ken Toba,[2] Kiminori Kato,[1] Takuya Ozawa,[1] Masato Oda,[1] Tsugumi Takayama,[1] Hironori Kobayashi,[2] Takao Yanagawa,[1] Haruo Hanawa,[1] Tomoyasu Suzuki,[1] Mikio Nakazawa,[3] Minoru Nomoto,[4] Fuyuki Asami,[5] Masato Higuchi,[6] Hideki Saito,[6] Yoshifusa Aizawa[1]

[1]Division of Cardiology, Niigata University Graduate School of Medical and Dental Sciences, Niigata, Japan, [2]Division of Hematology, Niigata University Graduate School of Medical and Dental Sciences, Niigata, Japan, [3]Division of Biomedical Sciences, Niigata University Graduate School of Medical and Dental Sciences, Niigata, Japan, [4]Division of Hepatology, Niigata University Graduate School of Medical and Dental Sciences, Niigata, Japan, [5]Division of Cardiac Surgery, Niigata University Graduate School of Medical and Dental Sciences, Niigata, Japan, [6]Product Research Department, Chugai Pharmaceutical Co., Ltd., Tokyo, Japan

Abstract

Erythropoietin (EPO) has long been utilized for the treatment of renal anemia. The erythropoietin receptor (EPOR) is also expressed in the cardiovascular and central nervous systems in addition to an erythroid lineage, to provide an organo-protective role against several types of cellular stress. Pulmonary hypertension (PH) is a poor prognostic disease caused by primary and secondary pulmonary vascular injury. We observed the effects of EPO derivatives on monocrotaline-induced PH in rats on the supposition that EPO may protect small arteries from injury. Asialoerythropoietin (AEPO) lacks sialic acids in the termini of carbohydrate chains that results in rapid clearance from blood. Carbamyl-erythropoietin (CEPO) interacts with EPOR/βc heterodimers, but not with EPOR homodimers expressed in erythroid cells. Monocrotaline-injected rats were treated with continuous intravenous injection of 2500 ng/kg/day of EPO, AEPO, or CEPO for 21 days, and lung histology, cardiac function, and mRNA expression in the lungs were examined. Wall thickening of small arteries in the lungs and PH were improved by administration of EPO, but not by its non-hematopoietic derivatives, AEPO, or CEPO. Erythropoietin administration increased mRNA expression of the anti-apoptotic molecule, Bcl-xL, and maintained expression of the CD31 antigen. We conclude that lungs may express EPOR homoreceptors, but not heteroreceptors. Adequate serum erythropoietin levels may be essential for pulmonary protective effects.

Keywords: pulmonary hypertension, monocrotaline, erythropoietin, asialoerythropoietin, carbamyl-erythropoietin

INTRODUCTION

Pulmonary hypertension (PH) is a serious disease caused by peculiar endothelial proliferation, plexiform lesions, and thickening of the tunica media as a result of smooth muscle cell (SMC) proliferation in arterioles and small arteries in the lungs (1). Most pulmonary hypertension is progressive and irreversible, except in rare cases with PH accompanied by bone marrow transplantation (2). Currently, standard treatment for this disease is administration of prostacyclins (3), calcium-channel blockers (4), phosphodiesterase type 5 inhibitors (5), and endothelin receptor antagonists (6), but 5-year survival rates are only 50% (7). Thus, new therapies are desirable.

Single-dose administration of monocrotaline, a phytoalkaloid, causes pulmonary endothelial damage followed by thickening of the tunica media, PH, and right ventricular hypertrophy, and has been utilized to reproduce experimental PH in animals (8).

Erythropoietin (EPO) is an erythroid hematopoietin secreted in the kidney in response to anemia and hypoxia. The erythropoietin receptor (EPOR) is expressed in immature erythroid cells, as well as the cardiovascular and central nervous systems to protect tissues from injury via its anti-apoptotic signal (9). In vitro administration of EPO inhibits hypoxia-induced apoptosis of endothelial cells (ECs) in culture via Akt1 and cysteine protease pathways (10). Erythropoietin also induces endothelial nitric oxide synthase (eNOS) activity and PI3K-dependent Bcl-xL production in cultured ECs (11,12).

In a previous study, conditional knockout (KO) mice of EPOR in non-hematopoietic tissue exhibited insufficient recruitment of endothelial progenitor cells (EPCs) with a decline in eNOS induction in the lungs in response to

Address correspondence to Ken Toba, MD, Division of Hematology, Niigata University Graduate School of Medical and Dental Sciences, 1-754 Asahimachi-dori, Chuo-ku, Niigata 951-8510, Japan. E-mail: tobaken@med.niigata-u.ac.jp

Received 5 February 2012; revised 15 March 2012; accepted 24 March 2012.

hypoxia (13). However, to the best of our knowledge, there has been only one report showing the direct effect of exogenously administered EPO on monocrotaline-induced PH (14,15). In that report, single-dose intraperitoneal bolus administration of EPO (10 μg/kg, Darbepoetin-α) decreased medial wall thickness of preacinar arteries, but did not improve pulmonary arterial hypertension or right ventricular hypertrophy (14). Single-dose administration of EPO may have been insufficient to protect small arteries from progressive EC injury caused by monocrotaline administration.

We previously reported on the tissue-protective effects of EPO on a limb ischemia model in mice (16), as well as on experimental autoimmune myocarditis in rats (17). We planned to examine the vasculoprotective effects of EPO on monocrotaline-induced PH in rats. Asialoerythropoietin (AEPO) and carbamyl-erythropoietin (CEPO) were also examined in comparison to native EPO. Asialoerythropoietin is a derivative of EPO lacking sialic acids in the termini of *N*- and *O*-glycans, and it expresses higher affinity to EPOR than EPO (18). Carbamyl-erythropoietin is another derivative of EPO that binds to the heterodimer of the EPOR and cytokine receptor common beta-chain (βc, CD131), but not to the homodimer of EPOR expressed in the hematopoietic system (19).

MATERIALS AND METHODS

All procedures were performed under sterile conditions with the approval of the Institutional Animal Care and Use Committee in compliance with the procedures and methods outlined by the Guide for the Care and Use of Laboratory Animals (NIH publication No. 85-23). The Animal Study Committee of our institution also approved the experimental projects.

Rat Model

Adult male Wistar rats (6–7 wk old) were obtained from Charles River Japan (Yokohama, Japan). Recombinant human erythropoietin (rhEPO) and asialoerythropoietin (rhAEPO, both provided by Chugai Pharmaceutical Co., Ltd., Tokyo, Japan) were adjusted to appropriate concentrations in RMPI1640 medium (Nipro, Tokyo, Japan), put into an Alzet mini-osmotic pump Model 2004 (Durect, Cupertino, CA, USA), connected to an Alzet Rat Jugular Catheter (Durect), and incubated for 48 hours at 37°C.

Rats were anesthetized by intraperitoneal administration of pentobarbital sodium (60 mg/kg). Left jugular veins were set with the catheter, and osmotic pumps were subcutaneously set on the back. Monocrotaline (Wako Chemicals, Osaka, Japan) was subcutaneously injected (80 mg/kg) at the same time as infusion of EPO derivatives was started. Monocrotaline-injected rats were intravenously injected continuously for 21 days with medium in the absence (medium group, $n = 9$) or presence of EPO derivatives (2500 ng/kg/day, EPO group: $n = 8$, AEPO group: $n = 9$) from osmotic pumps through the jugular catheter (rhEPO: 0.2 IU/ng). Normal rats ($n = 8$) were also examined for the measurements given below.

Catheter Examination

Rats were anesthetized by inhalation of 2% halothane (Dainippon Pharmaceutical Co., Osaka, Japan) on day 21 after monocrotaline administration, and physiologically examined during mechanical ventilation. For the measurement of aortic pressure, a polyethylene catheter (PE-50, Becton Dickinson, Parsippany, NJ, USA) was inserted into the right femoral artery, and a pressure transducer (P50, Gould Statham, Oxnard, CA, USA) was connected. Left and right ventricular pressures were measured using catheter tip transducers, one (Millar SPR407, Millar Instruments Inc., Houston, TX, USA) inserted into the right carotid artery and the other (Millar SPR671) into the right jugular vein, respectively. Heart rate (HR) was measured using an electrocardiogram on the body surface. All data were recorded using Power Lab/8sp (AS Instruments, Castle Hill, Australia).

Tissue Preparation

Rats were killed and blood samples were taken for the measurement of the blood cell count and serum EPO levels, and right lungs were immediately removed and washed with natural saline to obtain samples for quantitative real-time polymerase chain reaction (QRT-PCR). Total RNA was isolated from right lung samples with Trizol (Life Technologies, Tokyo, Japan) immediately after lung removal. Left lungs and hearts were simultaneously removed thereafter. Blood in the left lungs was removed by natural saline injected into the right ventricle and drained from the left atrium. Right and left ventricles plus septa were weighed separately to determine the ratio (RV/LV + S) as an index of right ventricular hypertrophy. Left lungs were then fixed using 10% formalin injected into the trachea, removed, fixed overnight, and embedded in paraffin for histological examination. A cross section (6 μm thick) on the hilum level was put on a slide; paraffin was removed, and then stained with hematoxylin–eosin. Pulmonary arteries of 50–200 μm (outside diameter) were observed using a System Life Microscope (BHS, Olympus, Japan) installed with an ocular micrometer, and the wall thickness (ratio) was estimated using Matsuda's method, that is, ratio of wall thickness (outside diameter – inner diameter) to the outside diameter (20). Spleens were also removed to measure their weight.

Additional In Vivo Experiments of CEPO Administration

Another erythropoietin derivative CEPO became available later, and we planned additional in vivo experiments using a monocrotaline-induced rat PH model in the same manner to determine the type of EPOR in the lung: EPOR homoreceptors or EPOR/βc heteroreceptors. Monocrotaline-injected rats were administered continuously for 21 days with medium ($n = 6$) or

rhCEPO (Chugai, 2500 ng/kg/day, $n = 8$), and examinations of blood, catheter, and lung histology were done. Carbamyl-erythropoietin did not react with the EPO enzyme-linked immunosorbent assay (ELISA) system.

ELISA and Quantitative Real-Time Polymerase Chain Reaction

Human erythropoietin, rat erythropoietin, and rat vascular endothelial growth factor (VEGF) levels in blood were measured using an ELISA method (R&D Systems, Minneapolis, MN, USA). The mouse/rat erythropoietin enzyme-linked immunosorbent assay system detected rat EPO, as well as rhEPO and rhAEPO, but not rhCEPO. The human erythropoietin enzyme-linked immunosorbant assay system also detected rhEPO and rhAEPO, but not rhCEPO.

Primers for mRNA detection are shown in Table 1. Quantitative real-time polymerase chain reaction was performed as previously described (21). Rat γ-actin was measured as an internal standard, and mRNA expression levels were indicated as relative copy number/internal standard. Templates for quantitative real-time polymerase chain reaction were fashioned as control genes to produce standard concentration curves. cDNA and diluted recombinant plasmids were measured using LightCycler (Roche, Indianapolis, IN, USA) and its software. After initial denaturation for 30 minutes at 95°C, a three-step cycle procedure was used (denaturation at 95°C for 5 s, annealing at 60°C for 15 s, and then extension and acquisition at 72°C for 13 s).

Statistical Analysis

The results of in vivo studies were compared among the four groups by a one-way analysis of variance (ANOVA) followed by Tukey's multiple comparison tests. The results of additional in vivo studies were compared between the two groups by unpaired t-tests. Differences were considered as significant at a P value of $<.05$.

RESULTS

In Vivo Hematopoiesis

Thirty-four rats, including normal rats ($n = 8$) and monocrotaline-injected rats, were analyzed (Figure 1).

Table 1. Primers for rat QRT-PCR

	Sense primer	Antisense primer
Rat γ-actin	5′-gaccttccttccgggcatggagt-3′	5′-tggaggggcctgactcgtcatact-3′
Rat eNOS	5′-tatttccaaggaagttacagagcc-3′	5′-tatggttacagatgtaggtgaaca-3′
Rat ET-1	5′-gatccttgaaagacttacttccca-3′	5′-ctgtagagttccgctttcaacttt-3′
Rat Bcl-xL	5′-tacaagctctcccagaaaggatac-3′	5′-atcccgaaagaattcattcactac-3′
Rat Bcl-2	5′-tataagctgtcacagaggggctac-3′	5′-ctgactggacatctctgcaaagtc-3′
Rat CD31 (PECAM-1)	5′-ctcctaagagcaaagagcaacttc-3′	5′-ccctcctttttctttgtaaaactga-3′
Rat CD45 (LCA)	5′-gcatgaactagagatgagcaaaga-3′	5′-gcagaatataggctgaggatttgt

Abbreviation: QRT-PCR – quantitative real-time polymerase chain reaction.

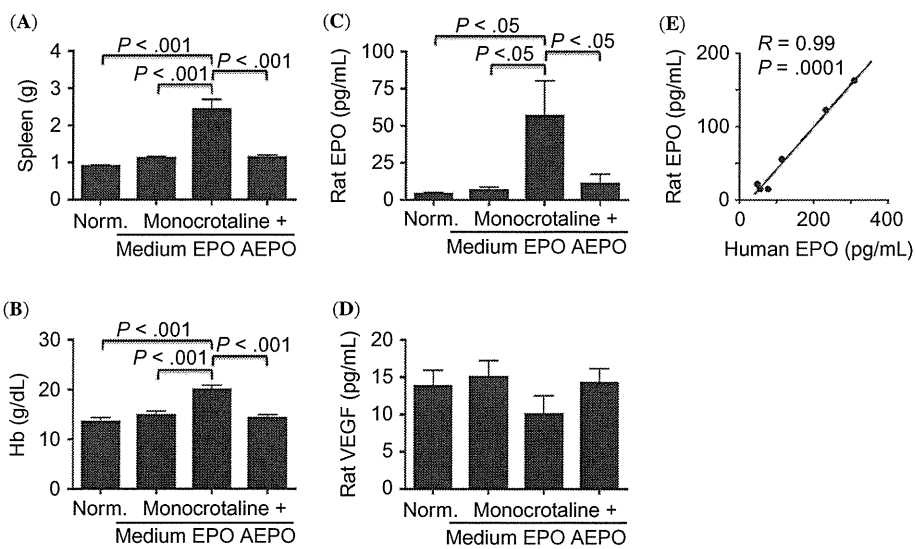

Figure 1. Hematological examinations in rats. Monocrotaline-injected (im) rats were treated with continuous administration (iv) of 2500 ng/kg/day of EPO, AEPO, or medium for 21 days and were compared with normal rats. Spleen size (**A**), hemoglobin level (**B**), serum EPO level (**C**), and the serum VEGF level (**D**) are shown. Note that the rat EPO ELISA system cross-reacts with human EPO. Serum erythropoietin levels were also analyzed by a human EPO ELISA system in six of eight rats in the EPO group (**E**). R in panel (**E**): Pearson's correlation efficient. Abbreviations: EPO – erythropoietin; AEPO – asialoerythropoietin; VEGF – vascular endothelial growth factor; ELISA – enzyme-linked immunosorbent assay.

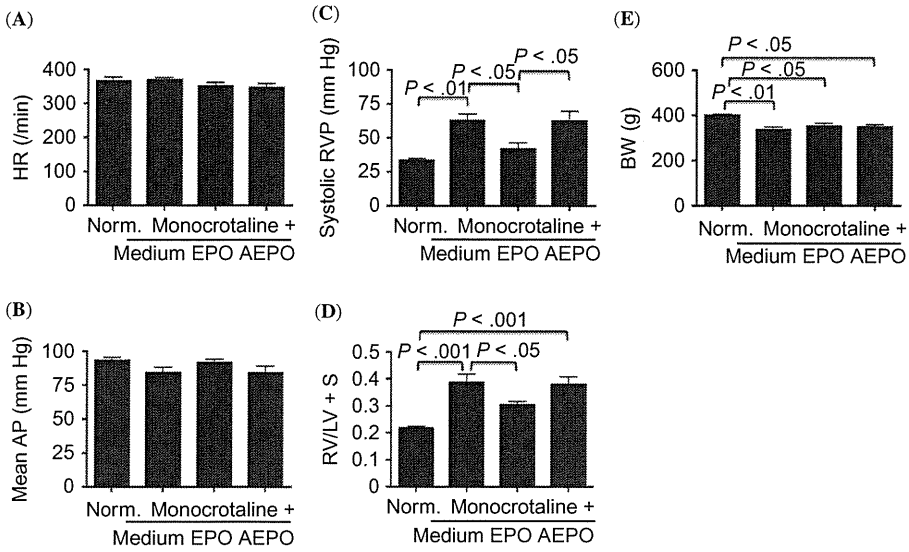

Figure 2. Cardiological examinations in rats. Monocrotaline-injected (im) rats were treated with continuous administration (iv) of 2500 ng/kg/day of EPO, AEPO, or medium for 21 days, and cardiac function was analyzed by catheter examination. Right ventricular weight was also measured after dissection and was normalized for total BW. HR (**A**), mean AP (**B**), peak RVP (**C**), right ventricular weight/left ventricle + septum weight (RV/LV + S) (**D**), and BW (**E**) are shown. Abbreviations: EPO – erythropoietin; AEPO – asialoerythropoietin; BW – body weight; HR – heart rate; AP – aortic pressure; RVP – right ventricular pressure.

Monocrotaline-injected rats underwent continuous infusion of medium ($n = 9$) or medium with 2500 ng/kg/day of rhEPO ($n = 8$), or rhAEPO ($n = 9$). Administration of erythropoietin, but not AEPO, increased hemoglobin levels and spleen weights. An increase in serum EPO levels was observed after administration of EPO, but not after AEPO. Serum levels of rat EPO and human EPO in the EPO group were 65.5 ± 63.3 and 139.7 ± 106.9 pg/mL, respectively. Data from the two ELISA system experiments correlated very well ($R = 0.99$, $P < .0001$). Serum vascular endothelial growth factor levels did not change.

Cardiac Function

Data from catheter examinations are shown in Figure 2. No differences were observed in HRs or mean aortic pressures among the four groups. Monocrotaline administration significantly induced a rise in the peak right ventricular pressure. The rise in peak right ventricular pressure was inhibited by administration of EPO, but not by AEPO. Monocrotaline administration significantly induced an increase in the RV/LV + S weight ratio, as well as a loss in body weight. The increase in RV/LV + S was inhibited by administration of EPO, but not by AEPO.

Histological Examination of the Lungs

No difference was observed in the inner diameter of pulmonary small arteries among the four groups (Figure 3). Wall thickening caused by medial hypertrophy was observed in the three monocrotaline-injected groups. Wall thickening was significantly prevented by administration of EPO, but not by AEPO.

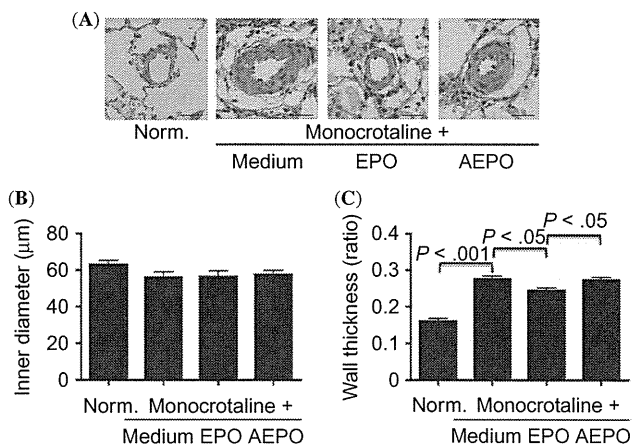

Figure 3. Lung histology in rats. Lung specimens were stained with HE (**A**) (magnification: ×400, scale bars = 50 μm), and 20 pulmonary arteries were measured for each specimen. The wall thickness (ratio) (**C**) was calculated from the inner diameter (**B**) and outer diameter of vessels. Abbreviation: HE – hematoxylin–eosin.

RNA Expression in the Lungs

Expressions of apoptosis regulators Bcl-2 and Bcl-xL, platelet EC adhesion molecule-1 (PECAM-1, CD31), endothelium-derived vasoconstrictor endothelin-1 (ET-1), eNOS, and leukocyte common antigen (LCA, CD45) were measured (Figure 4). Among the six molecules, endothelium-derived molecules, PECAM-1, and ET-1 decreased in the lungs due to monocrotaline administration and the decrease was prevented by continuous administration of EPO. Bcl-xL increased due to EPO. Like Bcl-xL, there was a trend for an increase in

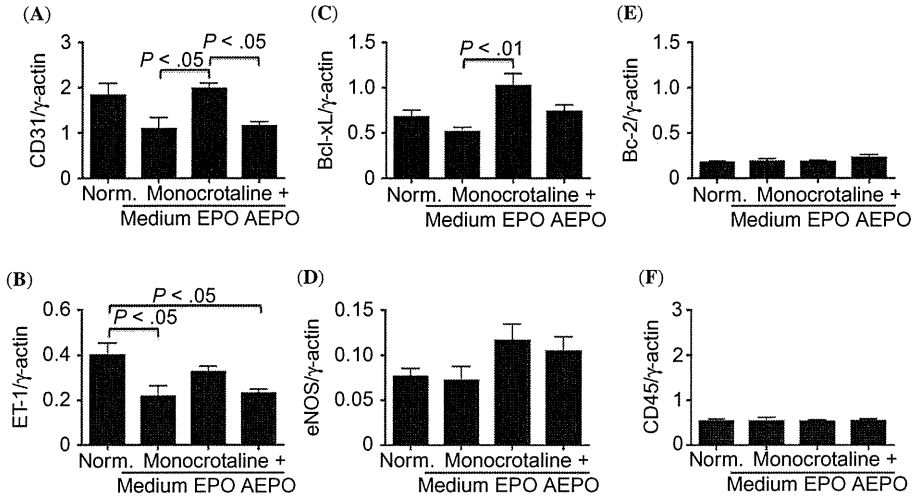

Figure 4. mRNA expression in the lungs of rats. Expression of mRNA in the lungs was measured, and expressed as relative copy number/γ-actin. (**A**) CD31 (PECAM-1); (**B**) endothelin (ET-1); (**C**) anti-apoptotic protein of ECs, Bcl-xL; (**D**) eNOS; (**E**) anti-apoptotic protein of leukocytes, Bcl-2; (**F**) leukocyte common antigen, CD45. Abbreviations: ECs – endothelial cells; eNOS – endothelial nitric oxide synthase; EPO – erythropoietin; AEPO – asialoerythropoietin.

eNOS expression due to EPO administration; however, this was not significant. No difference was observed in the expression of the leukocyte-derived molecules, CD45 and Bcl-2.

In Vivo Activity of CEPO

The results from CEPO administration are shown in Figure 5. Monocrotaline-administered rats underwent continuous infusion of medium (n = 6) or medium with 2500 ng/kg/day of rhCEPO (n = 8). No hematopoietic activity was observed by administration of CEPO in terms of hemoglobin levels or spleen weights. Carbamyl-erythropoietin administration did not prevent the rise in peak right ventricular pressure, increases in the RV/LV + S weight ratio, or wall thickening of pulmonary arteries caused by monocrotaline.

DISCUSSION

In this study, enlargement of the spleen was observed along with increases in hemoglobin levels. Extramedullar erythropoiesis is usually observed in spleens of mice and rats; therefore, simultaneous elevations in hemoglobin levels and spleen sizes were caused by hypererythropoiesis. The enzyme-linked immunosorbent assay system for EPO equally detects rhEPO and rhAEPO; nevertheless, an increase in serum EPO levels was not observed after infusion of AEPO. A clearance system of

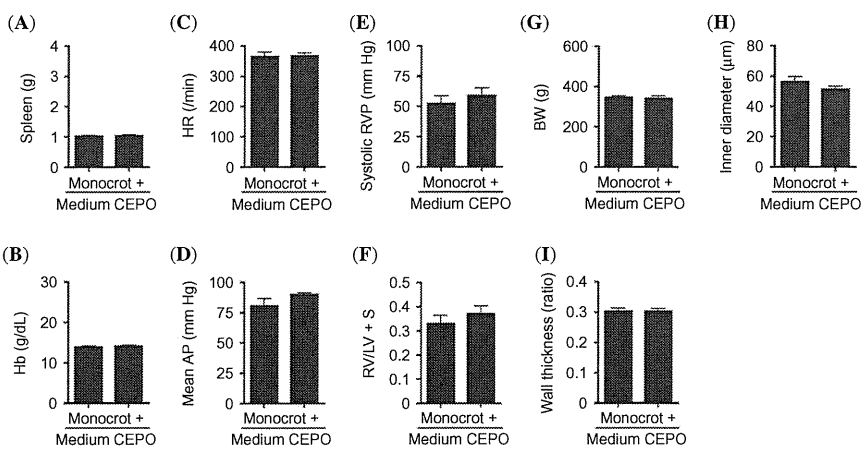

Figure 5. In Vivo effect of CEPO. Another set of in vivo experiments using CEPO was carried out in the same manner. Monocrotaline-injected (im) rats were treated with continuous administration (iv) of 2500 ng/kg/day of CEPO or medium for 21 days. Spleen size (**A**), hemoglobin level (**B**), HR (**C**), mean AP (**D**), peak RVP (**E**), right ventricular weight/left ventricle + septum weight (RV/LV + S) (**F**), BW (**G**), inner diameter (**H**), and wall thickness (ratio) (**I**) of small pulmonary arteries are shown. Abbreviations: CEPO – carbamyl-erythropoietin; HR – heart rate; AP – aortic pressure; RVP – right ventricular pressure; BW – body weight.

asialoglycoprotein, galactose receptors, exists in the liver (22) and intravenously injected AEPO possibly did not maintain its level in blood. Asialoerythropoietin administration also did not modify changes in cardiac function or pulmonary small arteries caused by monocrotaline, presumably due to the absence of an increase in serum levels. In panel (**E**) of Figure 1, data from the two ELISA systems completely correlated; thus, EPO levels in rats were due to the administration of rhEPO, and not from intrinsic rat EPO.

Erythropoietin promotes survival of primary human ECs through upregulation of Bcl-xL in vitro (11). In this study, it was suspected that continuous administration of EPO may exhibit pulmonary arterial endothelium protection from monocrotaline-induced apoptosis presumably via Bcl-xL induction. The rise in peak right ventricular pressure and gain in right ventricular weight caused by monocrotaline administration were significantly inhibited by administration of EPO. Therefore, erythropoietin administration may lead to improved right ventricular hypertrophy caused by monocrotaline administration.

In this study, EPO infusion was simultaneously started with administration of monocrotaline. Therefore, it is not known whether EPO administration can reverse PH once initiated. The major role of EPO in the cardiovascular and central nervous systems is its anti-apoptotic effects on EPOR-positive cells (9), and thus a pulmonary protective effect of EPO against monocrotaline-induced endothelial damage was expected. We doubt whether EPO could reverse the damage accompanied by fibrosis and so on, once established.

The half-life of single-dose EPO does not exceed 24 hours (23). Single-dose administration of monocrotaline causes progressive pulmonary endothelial damage for more than a period of several weeks (8), and intravenous bolus administration of EPO does not improve pulmonary arterial hypertension (14). We attempted to treat monocrotaline-induced PH with a continuous intravenous injection of EPO. Continuously administered erythropoietin partially prevented the progression of monocrotaline-induced PH in this study.

Through the use of an in vivo PH model, continuous administration of EPO increased Bcl-xL in the lungs, restrained monocrotaline-induced reduction in PECAM-1 and ET-1, prevented thickening of the pulmonary arterial wall, and improved PH. Endothelial cell damage induces proliferation of vascular SMCs, and EC repair terminates SMC proliferation (24). In clinical pulmonary hypertension, EC injury also plays an important role in the onset and progression of this disease (25). Infusion of endothelial progenitor cells improved monocrotaline-induced PH in rats (26), and EPO administration-induced EPC mobilization from bone marrow (27); thus, in addition to the direct protective effect of EPO on EC, EPC mobilization may also contribute to vascular protection.

An increase in serum levels was not observed after infusion of AEPO, presumably because of its rapid clearance from the circulation. In fact, hematopoietic activity of AEPO was observed in vitro, but not in vivo (28). Endothelial cells are continuously exposed to blood; thus, sufficient AEPO blood levels are essential for its effects on ECs. Therefore, it was thought that this was the reason why AEPO administration did not prevent endothelial damage in vivo.

Erythropoietin is a glycoprotein composed of 165 amino acid residues and 4 carbohydrate chains, 3 *N*-glycans and 1 *O*-glycan. All the sugar chains terminate with sialic acid capping. Erythropoietin spontaneously loses sialic acids, and is eliminated from the blood via clearance by asialoglycoprotein receptors expressed in the liver (22). Asialoerythropoietin that expresses affinity to EPOR, however, lacks erythropoietic activity in vivo (28). In contrast to this study, intravenous administration of AEPO showed high neuroprotective and renoprotective activities (29,30). Thus, it is possible that AEPO may have high affinity to tissue components, and blood concentrations, not tissue concentrations, of EPO may be essential for the treatment of monocrotaline-induced PH.

It is not clear why CEPO administration did not prevent monocrotaline-induced PH. Both primitive erythroid progenitors and definitive hematopoietic progenitors, but not cardiac or central nervous cells, arise from the hemogenic endothelium, and hemangioblasts are the source of hemogenic endothelia and mature ECs in ontogenesis (31). It is possible that erythroid and ECs express the homodimer of EPOR, not the heterodimer of EPOR and βc, and CEPO does not express bioactivity on either erythroid or ECs.

CONCLUSIONS

Erythropoietin improved chemical-induced vascular injury in vivo. On the other hand, intravenous administration of the non-erythropoietic EPO derivatives, AEPO and CEPO, did not improve vascular injury. The lungs may express EPOR homoreceptors, but not heteroreceptors.

ACKNOWLEDGMENTS

The authors disclosed the acceptance of the following financial support for the research and/or authorship of this article: Grants-in-Aid for scientific research from The Ministry of Education in Japan (grant numbers 21590887, 19590856, and 17590714 to K.T.; 21590888 to T.O.; and 18590806 to K.K.).

Declaration of interest: The authors declared no conflicts of interest with respect to the authorship and/or publication of this article.

REFERENCES

[1] Fishman AP. Changing concepts of the pulmonary plexiform lesion. Physiol Res 2000; 49:485–492.

[2] Limsuwan A, Pakakasama S, Hongeng S. Reversible course of pulmonary arterial hypertension related to bone marrow transplantation. Heart Vessels 2011; 26:557–561.

[3] Galiè N, Manes A, Branzi A. Prostanoids for pulmonary arterial hypertension. Am J Respir Med 2003; 2:123–137.

[4] Sitbon O, Humbert M, Jaïs X, et al. Long-term response to calcium channel blockers in idiopathic pulmonary arterial hypertension. Circulation 2005; 111:3105–3111.

[5] Galiè N, Ghofrani HA, Torbicki A, et al. Sildenafil citrate therapy for pulmonary arterial hypertension. N Engl J Med 2005; 353:2148–2157.

[6] Chang SA, Jang SY, Ki CS, Kang IS, Kim DK. Successful bosentan therapy for pulmonary arterial hypertension associated with hereditary hemorrhagic telangiectasia. Heart Vessels 2011; 26:231–234.

[7] Newman JH, Fanburg BL, Archer SL, et al. Pulmonary arterial hypertension: future directions: report of a National Heart, Lung and Blood Institute/Office of Rare Diseases workshop. Circulation 2004; 109:2947–2952.

[8] Hilliker KS, Bell TG, Roth RA. Pneumotoxicity and thrombocytopenia after single injection of monocrotaline. Am J Physiol 1982; 242:H573–H577.

[9] Maiese K, Li F, Chong ZZ. New avenues of exploration for erythropoietin. JAMA 2005; 293:90–95.

[10] Chong ZZ, Kang JQ, Maiese K. Erythropoietin is a novel vascular protectant through activation of Akt1 and mitochondrial modulation of cysteine proteases. Circulation 2002; 106:2973–2979.

[11] Zhande R, Karsan A. Erythropoietin promotes survival of primary human endothelial cells through PI3K-dependent, NF-kappaB-independent upregulation of Bcl-xL. Am J Physiol Heart Circ Physiol 2007; 292:H2467–H2474.

[12] Beleslin-Cokic BB, Cokic VP, Yu X, Weksler BB, Schechter AN, Noguchi CT. Erythropoietin and hypoxia stimulate erythropoietin receptor and nitric oxide production by endothelial cells. Blood 2004; 104:2073–2080.

[13] Satoh K, Kagaya Y, Nakano M, et al. Important role of endogenous erythropoietin system in recruitment of endothelial progenitor cells in hypoxia-induced pulmonary hypertension in mice. Circulation 2006; 113:1442–1450.

[14] van Albada ME, du Marchie Sarvaas GJ, Koster J, Houwertjes MC, Berger RM, Schoemaker RG. Effects of erythropoietin on advanced pulmonary vascular remodelling. Eur Respir J 2008; 31:126–134.

[15] Umar S, Steendijk P, Ypey DL, et al. Novel approaches to treat experimental pulmonary arterial hypertension: a review. J Biomed Biotechnol 2010; 2010:702836.

[16] Ozawa T, Toba K, Kato K, et al. Erythroid cells play essential roles in angiogenesis by bone marrow cell implantation. J Mol Cell Cardiol 2006; 40:629–638.

[17] Mitsuma W, Ito M, Kodama M, et al. Cardioprotective effects of recombinant human erythropoietin in rats with experimental autoimmune myocarditis. Biochem Biophys Res Commun 2006; 344:987–994.

[18] Dong YJ, Kung C, Goldwasser E. Receptor binding of asialoerythropoietin. J Cell Biochem 1992; 48:269–272.

[19] Brines M, Grasso G, Fiordaliso F, et al. Erythropoietin mediates tissue protection through an erythropoietin and common beta-subunit heteroreceptor. Proc Natl Acad Sci USA 2008; 101:14907–14912.

[20] Matsuda Y, Hoshikawa Y, Ameshima S, et al. Effects of peroxisome proliferator-activated receptor gamma ligands on monocrotaline-induced pulmonary hypertension in rats. Nihon Kokyuki Gakkai Zasshi 2005; 43:283–288.

[21] Yoshida T, Hanawa H, Toba K, et al. Expression of immunological molecules by cardiomyocytes and inflammatory and interstitial cells in rat autoimmune myocarditis. Cardiovasc Res 2005; 68:278–288.

[22] Weigel PH, Yik JH. Glycans as endocytosis signals: the cases of the asialoglycoprotein and hyaluronan/chondroitin sulfate receptors. Biochim Biophys Acta 2002; 1572:341–363.

[23] McMahon FG, Vargas R, Ryan M, et al. Pharmacokinetics and effects of recombinant human erythropoietin after intravenous and subcutaneous injections in healthy volunteers. Blood 1990; 76:1718–1722.

[24] Nasuno A, Toba K, Ozawa T, et al. Expression of coxsackievirus and adenovirus receptor in neointima of the rat carotid artery. Cardiovasc Pathol 2004; 13:79–84.

[25] Runo JR, Loyd JE. Primary pulmonary hypertension. Lancet 2003; 361:1533–1544.

[26] Zhao YD, Courtman DW, Deng Y, Kugathasan L, Zhang Q, Stewart DJ. Rescue of monocrotaline-induced pulmonary arterial hypertension using bone marrow-derived endothelial-like progenitor cells: efficacy of combined cell and eNOS gene therapy in established disease. Circ Res 2005; 96:442–450.

[27] Heeschen C, Aicher A, Lehmann R, et al. Erythropoietin is a potent physiologic stimulus for endothelial progenitor cell mobilization. Blood 2003; 102:1340–1346.

[28] Imai N, Higuchi M, Kawamura A, et al. Physicochemical and biological characterization of asialoerythropoietin. Suppressive effects of sialic acid in the expression of biological activity of human erythropoietin in vitro. Eur J Biochem 1990; 194: 457–462.

[29] Erbayraktar S, Grasso G, Sfacteria A, et al. Asialoerythropoietin is a nonerythropoietic cytokine with broad neuroprotective activity in vivo. Proc Natl Acad Sci USA 2003; 100:6741–6746.

[30] Yokomaku Y, Sugimoto T, Kume S, et al. Asialoerythropoietin prevents contrast-induced nephropathy. J Am Soc Nephrol 2008; 19:321–328.

[31] Lancrin C, Sroczynska P, Serrano AG, et al. Blood cell generation from the hemangioblast. J Mol Med 2010; 88:167–172.

Cardiovasc Drugs Ther (2012) 26:217–226
DOI 10.1007/s10557-012-6381-5

H_2 Mediates Cardioprotection Via Involvements of K_{ATP} Channels and Permeability Transition Pores of Mitochondria in Dogs

Akemi Yoshida · Hiroshi Asanuma · Hideyuki Sasaki · Shoji Sanada · Satoru Yamazaki · Yoshihiro Asano · Yoshiro Shinozaki · Hidezo Mori · Akito Shimouchi · Motoaki Sano · Masanori Asakura · Tetsuo Minamino · Seiji Takashima · Masaru Sugimachi · Naoki Mochizuki · Masafumi Kitakaze

Published online: 17 April 2012

Abstract
Purpose Inhalation of hydrogen (H_2) gas has been shown to limit infarct size following ischemia-reperfusion injury in rat hearts. However, H_2 gas-induced cardioprotection has not been tested in large animals and the precise cellular mechanism of protection has not been elucidated. We investigated whether opening of mitochondrial ATP-sensitive K+ channels (mK_{ATP}) and subsequent inhibition of mitochondrial permeability transition pores (mPTP) mediates the infarct size-limiting effect of H_2 gas in canine hearts.
Methods The left anterior descending coronary artery of beagle dogs was occluded for 90 min followed by reperfusion for 6 h. Either 1.3% H_2 or control gas was inhaled from 10 min prior to start of reperfusion until 1 h of reperfusion, in the presence or absence of either 5-hydroxydecanoate (5-HD; a selective mK_{ATP} blocker), or atractyloside (Atr; a mPTP opener).
Results Systemic hemodynamic parameters did not differ among the groups. Nevertheless, H_2 gas inhalation reduced infarct size normalized by risk area (20.6±2.8% vs. control gas 44.0±2.0%; $p<0.001$), and administration of either 5-HD or Atr abolished the infarct size-limiting effect of H_2 gas (42.0±2.2% with 5-HD and 45.1±2.7% with Atr; both $p<0.001$ vs. H_2 group). Neither Atr nor 5-HD affected infarct size per se. Among all groups, NAD content and the number of apoptotic and 8-OHdG positive cells was not significantly different, indicating that the cardioprotection

A. Yoshida · H. Sasaki · S. Yamazaki · M. Asakura · M. Kitakaze (✉)
Department of Cardiovascular Medicine, National Cerebral and Cardiovascular Center, Suita 565-8565, Osaka, Japan
e-mail: kitakaze@zf6.so-net.ne.jp

H. Asanuma
Department of Cardiovascular Science and Technology, Kyoto Prefectural University of Medicine, Suita 565-8565, Osaka, Japan

A. Yoshida · N. Mochizuki
Department of Structural Analysis, National Cerebral and Cardiovascular Research Center, Suita, Japan

S. Sanada · Y. Asano · T. Minamino · S. Takashima
Department of Cardiovascular Medicine, Osaka University Graduate School of Medicine, Suita, Japan

Y. Shinozaki · H. Mori
Department of Physiological Science, Tokai University Graduate School of Medicine, Isehara, Japan

A. Shimouchi
Department of Cardiac Physiology, National Cerebral and Cardiovascular Research Center, Suita, Japan

M. Sano
Department of Cardiology, Keio University School of Medicine, Tokyo, Japan

M. Sugimachi
Department of Cardiovascular Dynamics, Research Institute, National Cerebral and Cardiovascular Center, Suita, Japan

afforded by H_2 was not due to anti-oxidative actions or effects on the NADH dehydrogenase pathway.
Conclusions Inhalation of H_2 gas reduces infarct size in canine hearts via opening of mitochondrial K_{ATP} channels followed by inhibition of mPTP. H_2 gas may provide an effective adjunct strategy in patients with acute myocardial infarction receiving reperfusion therapy.

Key words Hydrogen gas · Reperfusion injury · Myocardial infarction · Mitochondrial K_{ATP} channel · Mitochondrial permeability transition pore

Introduction

Myocardial infarction (MI) is a leading cause of death worldwide, and reduction of infarct size is an important therapeutic goal for patients with acute MI (AMI). The prognosis of AMI has been improved dramatically due to the development of both catheterization techniques and reperfusion therapy by coronary mechanical methods or pharmacological intervention. However, strategies to limit reperfusion injury and thus infarct size have not been well applied in clinical settings [1, 2]. We reported that carperitide limited infarct size in a large scale clinical trial [3]; however, infarct size was reduced by only 14.7%, and the discovery of other therapeutics to limit infarct size may be clinically useful. Interestingly, hydrogen (H_2) has been reported to provide therapeutic benefit for many diseases related to oxidative stress, including cardiovascular disease. There is some evidence that inhalation of H_2 gas limits myocardial infarct size in rats [4, 5]. However, since heart physiology differs significantly in small animals relative to large animals and humans, it cannot be assumed that H_2 would limit infarct size in large animals and humans. Furthermore, the cellular mechanisms underlying H_2-mediated cardioprotection have not been clarified.

Recent accumulated evidence regarding cardioprotection afforded by ischemic pre- or post-conditioning has culminated in the idea that opening of mitochondrial ATP-sensitive K^+ channels (mK_{ATP}) followed by inhibition of mitochondrial permeability transition pores (mPTP) plays a central role in limiting infarct size [6–8]. Indeed, Piot et al. [9] found that administration of the mPTP inhibitor, cyclosporine, at the time of reperfusion limited the size of myocardial infarction in patients with AMI. Ohsawa et al. [10] demonstrated that H_2 has the potential to serve as an antioxidant in preventive and therapeutic applications. Oxygen-derived free radicals are generated inside and outside of cells, and H_2 gas can eliminate hydoxyradical and peroxynitrate because it can penetrate biomembranes and diffuse into the cytosol, mitochondria, and nuclei. If this is the case, H_2 gas may protect mK_{ATP} against ischemic injury, or may directly activate mK_{ATP} followed by the inhibition of mPTP.

Thus, we tested the hypothesis that H_2 gas may reduce reperfusion injury and limit infarct size via the activation of mK_{ATP} and the inhibition of mPTP.

Methods

Animal model and instrumentation

Fifty nine beagle dogs (Oriental Yeast Co., Ltd, Tokyo, Japan) weighing 9 to 10 kg were per-anesthetized with sodium pentobarbital (25 mg/kg iv). All dogs were rapidly intubated and anesthetized with analgesic anesthetics. The control or H_2 gas tank was connected to the respirator 10 min before reperfusion. After baseline hemodynamic assessment, thoracotomy was performed, and the left anterior descending coronary artery (LAD) was ligated just distal to the first diagonal branch. The left carotid artery was catheterized to monitor both aortic blood pressure and heart rate. At the end of each study, animals were euthanized with administration of a high dose of sodium pentobarbital. All procedures were performed in conformity with the Guide for the Care and Use of Laboratory Animals (NIH publication no. 85-23, 1996 revision).

Composition of gas mixture

Gas tanks were obtained from TAIYO NIPPON SANSO Corporation (Osaka, Japan). The control gas tanks were composed of 70% N_2 and 30% O_2. The H_2 gas tanks were composed of 1.3% H_2, 68.7% N_2, and 30% O_2. The H_2 gas concentration was set at 1.3% because higher concentrations create the possibility of explosion. Previous studies showed that 0.5%–4.0% H_2 limited infarct size in rat hearts in vivo, at a flow rate of 1 L/min.

Experimental protocols

After the randomization to either H_2 gas (n=18) or control gas (n=18), the LAD of the beagle was occluded for 90 min followed by reperfusion for 6 h. Either H_2 gas or control gas was inhaled (3.36 L/min) 10 min prior to reperfusion until 1 h of reperfusion. In addition, we intravenously administered either 5-hydroxydecanoate (5-HD, Sigma; 10 mg/kg i.v.), or atractyloside (Atr, Sigma; 2.5 mg/kg i.v.), for 5 min before gas inhalation [H_2 gas with 5-HD (n=6) or Atr (n=6) and control gas with 5-HD (n=6) or Atr (n=6)]. In all groups, infarct size was assessed after 6 h of reperfusion. We also investigated apoptosis in the myocardium adjacent to the infarct area using TUNEL staining. In addition, we counted the incidence of lethal arrhythmia, defined as more than 15 consecutive premature ventricular contractions (VPC) or ventricular fibrillation (Vf) from 10 min before reperfusion to 60 min after the onset of reperfusion.

Measurement of infarct size and myocardial collateral blood flow

We measured both area at risk and infarct area 6 h after the onset of reperfusion as described previously [11]. These parameters were evaluated by Evans blue and triphenyltetrazolium chloride (TTC) staining, respectively. Infarct size was calculated as [infarct area/area at risk] × 100(%).

Regional myocardial blood flow was determined by the microsphere technique. Non-radioactive microspheres (Sekisui Plastic Co., Ltd., Tokyo, Japan) are made of inert plastic labeled with niobium (Nb) and bromine (Br) as described in detail in previous study [12]. Microspheres were suspended in isotonic saline with 0.01% Tween80 to prevent aggregation. The microspheres were ultrasonicated for 5 min followed by 5 min of vortexing immediately before injection. Approximately 1 mL of the microsphere suspension ($2–4\times10^5$ spheres) was injected into the left atrium at 80 min after the start of coronary occlusion.

The X-ray fluorescence of stable heavy elements was measured by a wavelength dispersive spectrometer (PW 1480, PHILLIPS Co., Ltd.). The specifications of this X-ray fluorescence spectrometer have been described previously [12]. In brief, when the microspheres are irradiated by the primary X-ray beam, the electrons fall back to a lower orbit and emit measurable energy. The energy level of the X-ray fluorescence depends on the characteristics of each element. Therefore, it was possible to quantify the X-ray fluorescence of several differently labeled microspheres in the mixture. Regional myocardial collateral blood flow was calculated according to the following formula: time flow = (tissue count) × (reference flow)/(reference count), and was expressed in mL/g wet weight/min.

Terminal Deoxynucleotidyl transferase-mediated dUTP nick-end labeling (TUNEL)

The myocardial tissue samples were taken from the border zone of dogs in the control, H_2, control+5-HD, H_2+5-HD, control+Atr and H_2+Atr groups (n=3 each). The border zone was chosen as the region within 4 mm from the infarct zone. These were fixed in 10% buffered formalin, embedded in paraffin, and serially sectioned in the frontal plane at 5-μm thickness. To assess myocardial apoptosis, analysis by TUNEL method was performed according to the protocol supplied with the in situ apoptosis detection kit, the Apop Tag Peroxidase In Situ Apoptosis Detection Kit (S7100, MILLIPORE). The sections were then shortly counterstained with hematoxylin and eosin to visualize the cells. TUNEL-positive cell nuclei and total cell nuclei stained metylgreen were counted in 7–10 random high-power fields (×200). The amount of TUNEL-positive cells was expressed as a percentage of the total amount of cells (n=1,500).

Immunohistochemistry for either 8-OHdG or NAD+ of the Reperfused myocardium

The myocardial tissue samples were taken from the border zone between ischemic and non-ischemic areas in the control, H_2, H_2+5-HD, H_2+Atr, control+5-HD and control+Atr groups (n=3 each). After 90 min of ischemia followed by 6 h of reperfusion, hearts were excised and the myocardial tissue samples were taken from the border zone. The border zone was chosen as the region within 4 mm from the infarct zone. These were fixed in 10% buffered formalin, embedded in paraffin, and serially sectioned in the frontal plane at 5-μm thickness. The paraffin sections were deparaffinized in xylene, rehydrated using various grades of ethanol, and pretreated with 10 mM citric acid for 40 min at 95°C. For immunostaining, sections stained with anti-8OH-dG (MOG-020P; Japan Institute for the Control of Aging; 1:100) antibodies overnight at 4°C. Secondary antibodies conjugated Simple Stain Rat (MAX-PO MULTI 414191, NICHIREI Bioscience inc. Japan; undiluted) were applied for 30 min at room temperature. The sections were then shortly counterstained with hematoxylin and eosin to visualize the cells. Four slides were randomly examined using a defined rectangular field area with magnification (×40). The data were represented as the number of 8OH-dG positive cells per field.

Since mPTP may be opened via oygen-drived free radicals via the NADPH oxidase, we also investigated the myocardial NAD+ contents as well. We used 18 dogs for NAD assessment in the control, H_2, H_2+5-HD, H_2+Atr, control+5-HD and control+Atr groups (n=3 each). The myocardial tissue in the border zone was quickly placed into liquid nitrogen and stored at −80°C. For the measurement of NAD+, 40 mg of border zone tissue was homogenized. An equal amount of protein from the homogenized tissue of each group was used for the NAD+/NADH Colorimetric assay kit (Cat# CY-1253; Cyclex Co., Ltd).

Exclusion criteria

To ensure that all animals used in the present study were healthy and had been exposed to a similar extent of ischemia, the following standards were employed for the exclusion of unsatisfactory dogs: (1) subendocardial collateral blood flow greater than 15 mL/100 g/min; (2) heart rate greater than 170 beats/min; and (3) more than two consecutive attempts required to terminate ventricular fibrillation (Vf) using low-energy DC pulses applied directly to the heart.

Statistical analysis

Statistical analysis was performed using two-way repeated measures analysis of variance (ANOVA) when data were

compared over the time course of the change between groups. Analysis of covariance between regional collateral flow in the inner half of the left ventricular wall and infarct size was described previously [11]. Other data were compared using one-way fractional analysis of variance. If statistical significance was found for a group, time effect, or group-by-time interaction, further comparisons were made with paired t tests between all possible pairs of the five groups at individual time points. Results were expressed as means ± SEM, with $p<0.05$ considered statistically significant.

Results

Among the 59 dogs, 23 were excluded due to Vf or excessive myocardial collateral blood flow (>15 mL/100 g/min). The remaining 36 dogs completed the protocols satisfactorily and were included in the data analysis. None of the pharmacological interventions such as H_2 gas, control gas, 5-HD, or Atr, altered systemic blood pressure or heart rate during the experimental protocols (Table 1).

Inhalation of H_2 gas just prior to reperfusion following 90 min of ischemia reduced infarct size normalized by risk area (20.6±2.8% vs. 44.0±2.0%; $p<0.001$) (Fig. 1). Intriguingly, the administration of either 5-HD or atractyloside (Atr) blunted the H_2 gas induced limiting effect on infarct size (42.0 ±2.2% in 5-HD vs. 45.1±2.7% in Atr; $p<0.001$ and $p<0.001$ vs. H_2 gas group). Neither 5-HD nor atractyloside per se affected infarct size. There were no differences in either risk area or collateral flow during the ischemic period among the groups (Fig. 2). Figure 3 shows the regression plots of the area at risk vs. collateral flow. Inhalation of H_2 gas mediated the substantial cardioprotection irrespective of collateral flow, which was again blunted by either 5-HD or atractyloside.

On the other hand, we observed apoptosis using TUNEL staining in the myocardium in each group; there were no differences in the extent of apoptosis in the groups (36.0± 1.8, 26.5±6.9, 33.0±1.4, 35.6±1.5, 35.0±1.3 and 35.7±1.4% in the control group, the H_2 gas group, the H_2 gas with 5HD group, the H_2 gas with Atr group, the control gas with 5HD group, and the control gas with Atr group, respectively).

We observed the incidence of lethal arrhythmia throughout the experiments in all groups from 10 min before reperfusion to 60 min after the onset of reperfusion (Table 2). The presence of either Vf or VPC longer than 15 consecutive beats was defined as lethal arrhythmia in this study. The incidence of lethal arrhythmia in the reperfusion period tended to decrease by H_2 gas although there were no significant differences. This tendency was blunted by either 5-HD or Atr. These data indicate that H_2 gas may affect the incidence of fatal ventricular arrhythmias during the reperfusion period, but it is unknown whether this effect is attributable to a potential primary anti-arrhythmic effect of H_2 gas or merely secondary to the infarct size-limiting effects of H_2 gas.

The number of 8-OHdG (a biomarker of oxidative stress) positive cells, tended to decrease in H_2 group relative to the other groups, however there was no significant difference (Fig. 4). We also observed no relation between the number

Table 1 Effect of H_2 gas on systemic hemodynamic parameters

Groups	Baseline	Isc-60	Isc-90	Rep-60	Rep-120	Rep-180	Rep-240	Rep-300	Rep-240
Mean blood pressure (mmHg)									
Control gas	101±2	103±2	104±2	98±2	102±2	101±3	103±3	99±3	100±2
H_2 gas	105±4	97±2	98±3	96±3	100±2	101±3	99±2	101±2	103±1
H_2 gas + 5HD	105±2	105±2	106±1	95±3	98±3	101±3	103±1	102±0	100±4
H_2 gas + Atr	98±3	98±3	102±3	98±1	100±1	101±1	102±1	102±2	103±1
Control gas + 5HD	104±2	101±2	101±1	102±2	103±2	101±3	103±2	98±3	100±4
Control gas + Atr	102±1	102±4	100±2	96±1	103±2	100±3	103±2	104±2	102±1
Heart rate (beats/min)									
Control gas	136±3	138±2	137±2	132±2	131±1	135±3	135±4	133±4	133±4
H_2 gas	139±3	138±3	140±4	133±3	134±4	134±5	134±4	134±5	132±4
H_2 gas + 5HD	135±3	130±3	129±4	129±3	129±4	130±3	129±4	129±4	130±3
H_2 gas + Atr	134±2	135±4	130±4	129±3	129±2	129±3	129±2	128±3	129±3
Control gas + 5HD	134±4	135±3	135±3	135±2	129±3	131±5	132±5	130±5	129±5
Control gas + Atr	137±2	137±2	135±3	136±2	137±3	135±4	135±2	135±3	136±2

Values are expressed as mean ± SEM. Isc-60 and Isc-90 show 60 and 90 min after the onset of myocardial ischemia, respectively. Rep-60, Rep-120, Rep-180, Rep-240, Rep-300 and Rep-360 show 60, 120, 180, 240, 300 and 360 min after the onset of reperfusion, respectively. There were no significant changes of theses parameters among the six groups

5HD = 5-hydroxydecanoate; Atr = Atractyloside

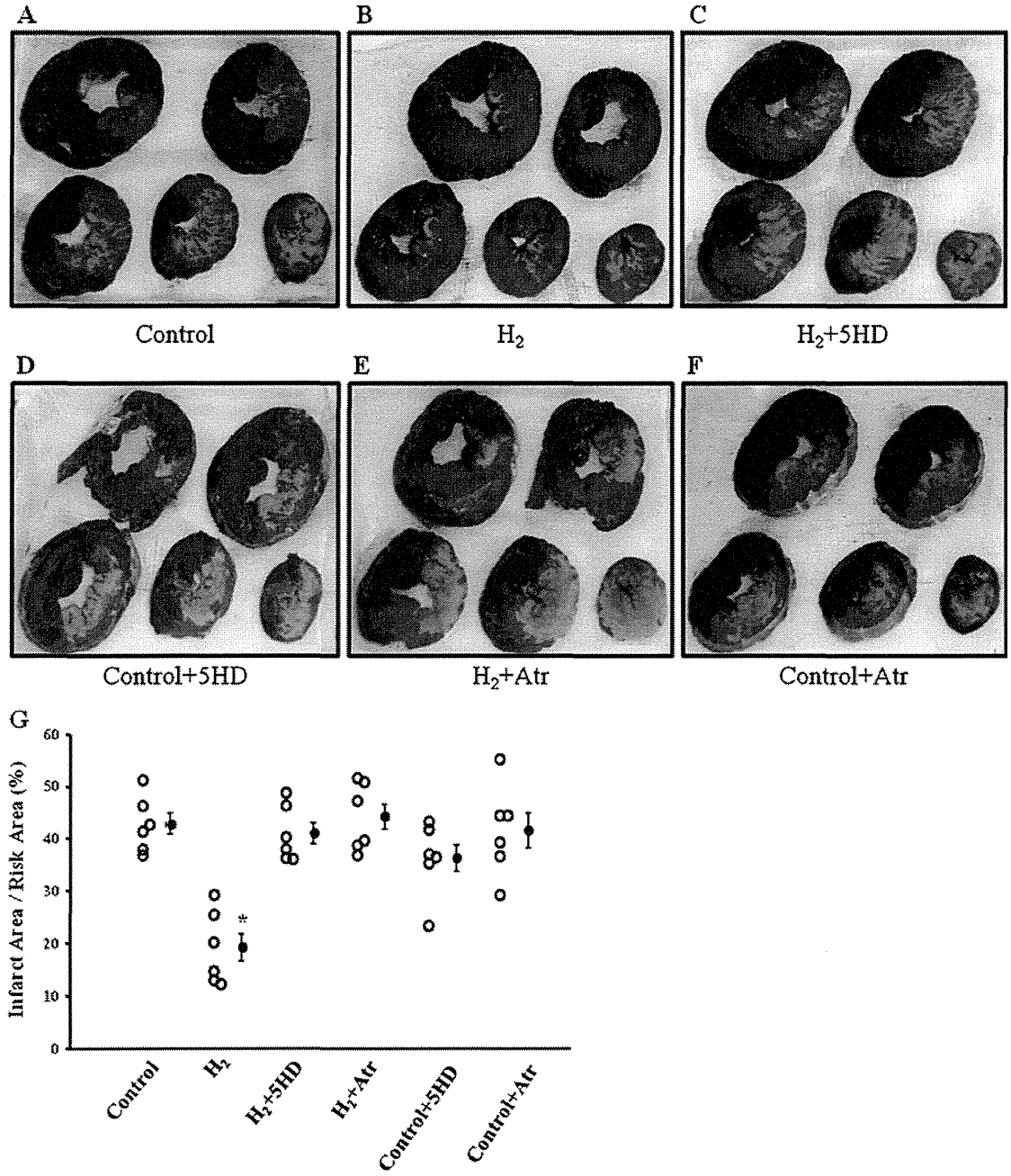

Fig. 1 Effect of H_2 Gas on Myocardial Infarct Size. Values are expressed as mean ± SEM (error bars). Representative photos following both Evans Blue and triphenyltetrazolium chloride staining are shown in the control gas (**A**), H_2 gas (**B**), H_2 gas with 5HD (**C**), H_2 gas with Atr (**D**), control gas with 5HD (**E**), and the control gas with Atr groups (**F**) respectively. **G** Myocardial infarct size quantification as a percentage of the area at risk in groups tested. Inhalation of hydrogen gas reduced infarct size. 5HD and Atr abolished this cardioprotective effect. *$p<0.0001$ vs. control group. 5HD = 5-hydroxydecanoate; Atr = atractyloside

of 8-OHdG positive cells and infarct size. We next investigated myocardial NAD+ levels and observed a not significant tendency towards increased NAD+ levels in the H_2 group, suggesting that the inhibition of mPTP caused by the opening of mK_{ATP} may not be attributable to oxygen-derived free radicals produced through NADH dehydrogenase (Fig. 5).

Discussion

The present study provides a novel finding that inhalation of H_2 gas mediates infarct size-limiting effects but not cellular apoptosis-limiting effects in the canine heart large animal model, and that H_2 gas-mediated cardioprotection is mainly attributable to the opening of mK_{ATP} followed by inhibition

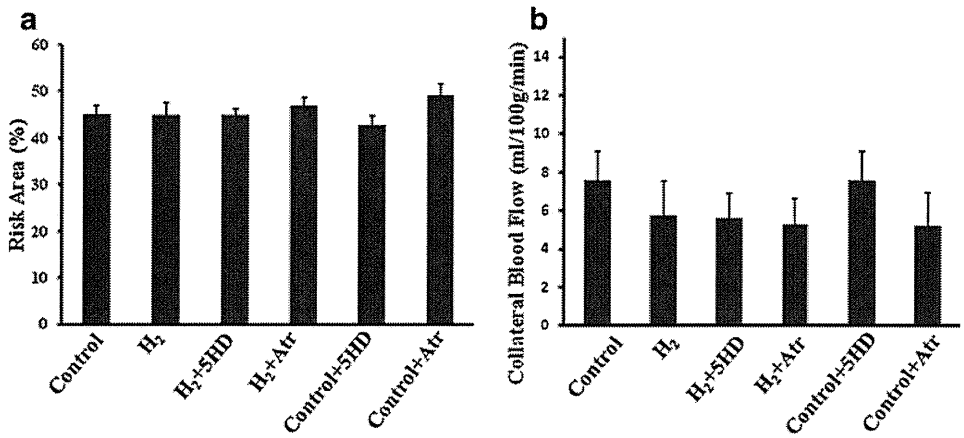

Fig. 2 Risk Area and Collateral Flow. Risk area (**a**) and collateral blood flow (**b**). There were no differences in either risk area or collateral blood flow in all groups. Values are expressed as mean ± SEM (error bars)

of mPTP, although we could not completely exclude the involvements of H_2 gas-mediated anti-oxidant effects on the present results.

Factors that affect infarct size during inhalation of H_2 gas

The infarct size-limiting effect of H_2 gas may be attributable to changes in systemic hemodynamics and/or collateral flow, because these two factors are critical in determining infarct size. However, when H_2 gas was inhaled, systemic blood pressure, heart rate, and collateral flow were unchanged among the groups. Therefore, H_2 gas-induced cardioprotection is not mediated by hemodynamic or collateral flow changes secondary to the inhalation of H_2 gas. Myocardial contractility is another determinant of infarct size, since increases in myocardial contractility may increase infarct size; indeed, beta blockers, which reduce myocardial contractility, reduce infarct size. However, Hayashida et al. [5] and Sun et al. [4] showed that either H_2 gas or H_2-rich saline provokes no changes in myocardial contractility as a index of maximal dP/dt, suggesting that myocardial contractility is not altered by H_2 gas, although we did not measure myocardial contractility in the present study.

We have shown that H_2 gas limits infarct size in large animals, which may be translated to human use. In rats, heart rate and maximal dP/dt are around 400/min, and 8,000 mmHg/sec, respectively [5]. However, in the anesthetized dog, these parameters are around 130/min and 4,000 mmHg/sec, respectively [13, 14]. Therefore, the fact that H_2 gas limits infarct size in rat hearts does not necessarily indicate that this will be the case in large animals. We found cardioprotective effects of H_2 gas in canine hearts, indicating that potent cardioprotection by H_2 gas or H_2-rich saline may be the case for possible human use. However, in our large animal model, apoptosis was not prevented by H_2 gas, which is different from results seen by Sun et al. [4]. We

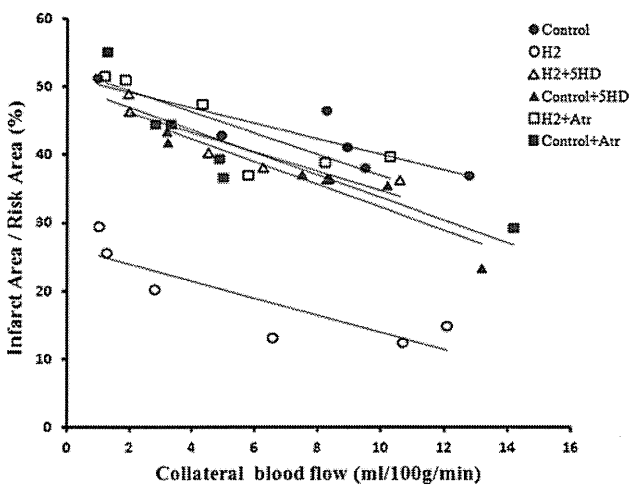

Fig. 3 Plot of infarct size expressed as a percentage of the risk area and regional collateral flow during ischemia. The abbreviations are same as in Fig. 1 There are inverse relations between normalized infarct area and collateral flow, and a significant difference ($P<0.05$) is seen in the H_2 gas group compared with the control group

Table 2 Incidence of lethal arrhythmia during ischemia and reperfusion periods and number of dogs excluded for lethal arrhythmia

Groups	Lethal arrhythmia		No. of excluded dogs	
	Ischemia period (counts)	Reperfusion period (counts)	Vf (counts)	Collateral blood flow (ml/100 g/min)
Control gas	0	23	1	3
H_2 gas	0	5	0	2
H_2 gas + 5HD	0	29	1	3
H_2 gas + Atr	0	27	1	3
Control gas + 5HD	0	28	2	2
Control gas + Atr	1	30	3	2

Incidence of lethal arrhythmia is shown in the included dogs of the present study. H_2 gas group tended to reduce incidence of lethal arrhythmia, however, there were no significant differences among the six groups. Vf = ventricular fibrillation; Abbreviations as in Table 1

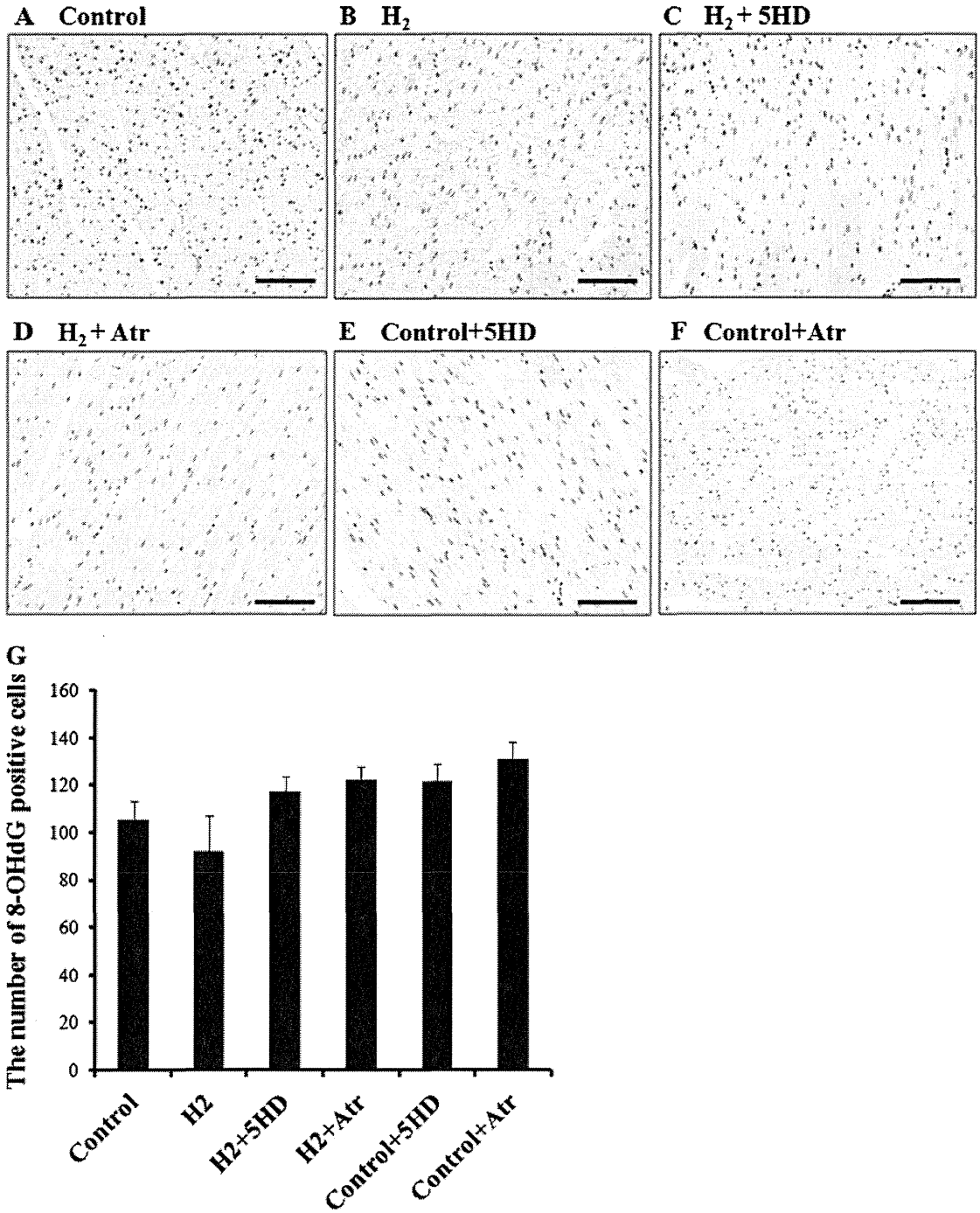

Fig. 4 The number of 8-OHdG positive cells. Representative photos assessed by 8-OHdG immunoreactivity. Staining was localized to nuclei of myocardium (brown) in the control gas (**A**), H_2 gas (**B**), H_2 gas with 5HD (**C**), H_2 gas with Atr (**D**), control gas with 5HD (**E**), and the control gas with Atr groups (**F**) respectively. Scale bar=100 μm. **G** The quantification of 8-OHdG positive cells was expressed per field. There were no significant differences among the six groups. Values are expressed as mean ± SEM (error bars)

did not determine the mechanisms underlying these differences. Since the mechanisms of myocardial necrosis and apoptosis are different [15], our results do not discourage the clinical use of H_2.

On the other hand, we also observed the tendency that H_2 gas mediates the inhibitory effect on reperfusion arrhythmias suggesting that H_2 gas may primarily inhibit reperfusion lethal arrhythmias, however, we cannot deny the

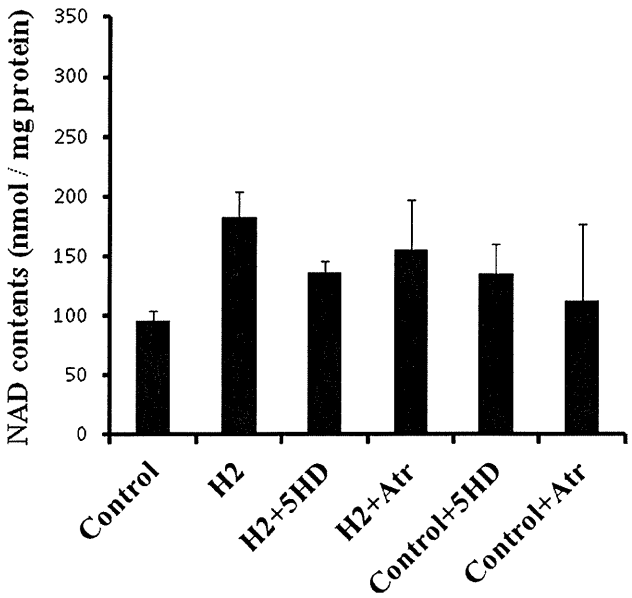

Fig. 5 The myocardial NAD contents. There were no significant differences of myocardial NAD contents among the six groups. Values are expressed as mean ± SEM (error bars)

possibility that this anti-arrhythmic effect of H_2 gas is secondary to the infarct size-limiting effect.

Cellular mechanisms of H_2 gas-induced cardioprotection

H_2 gas is reported to scavenge the detrimental, hydroxyl-radical and peroxynitrate reactive oxygen species without affecting less potent oxygen derived-free radicals or hydrogen peroxide [10]. This may afford cardioprotection by attenuating the end-products of ROS [5, 16–19]. However, this does not necessarily mean that removal of detrimental ROS is the sole mechanism by which H_2 gas induces cardioprotection. Indeed, we found no significant differences in myocardial 8-OHdG immunoreactivity (Fig. 4) among the six groups although there was a trend to lower 8-OHdG positive cells, suggesting that the current dose of H_2 gas may not provide anti-oxidant effects enough to potently reduce infarct size. In turn, we observed the alternative mechanism for H_2 gas to mediate cardioprotection, i.e., the activation of mK_{ATP} followed by the inhibition of mPTP during reperfusion following myocardial ischemia. It would be difficult for chemicals or endogenous substances to physically reach mK_{ATP} upon reperfusion, and the most important endogenous mediator of ischemic preconditioning, adenosine, opens mK_{ATP} via adenosine receptors, Gi proteins, and PKC pathways [20–23]. However, H_2 gas easily penetrates cells and reaches cellular substances and mitochondria [10], suggesting that H_2 gas can reach and activate mK_{ATP}. Another possibility is that H_2 gas activates PKC inside cells, and the activated PKC opens mK_{ATP}. The activation of mK_{ATP} is reported to transmit signals that inhibit mPTP [24–30], which causes potent cardioprotection. An additional finding was that no significant differences were shown in myocardial NAD+ contents although there was a trend to increase in H_2 group. The effects of H_2 gas to modulate either mKATP or mPTP are through a pathway other than NADH dehydrogenase, although there are data showing that the opening of mKATP increases ROS, which modulates mPTP and mediates cardioprotection.

Although we do not understand the precise mechanisms by which H_2 gas opens mK_{ATP}, the evidence in the present study suggests that H_2 gas stimulates intracellular signaling pathways of ischemic preconditioning or postconditioning of cardioprotection [31]. Since H_2 gas is produced in vivo [32], this mechanism may serve as a trigger or mediator of ischemic preconditioning. In turn, it is hard for basic and clinical researchers to translate the fruitful results of ischemic pre- or postconditioning to clinical outcomes. If H_2 gas-induced cardioprotection breaks into the sequels of the signal transduction of ischemic pre- or postconditioning, H_2 gas is likely to be used in clinical situations. Indeed, cyclosporine, which inhibits mPTP, has recently been shown to mediate potent cardioprotection in patients with acute myocardial infarction [9].

Translation to clinical medicine

Before considering the translation of the present results to clinical settings, we need to consider several issues. First, we used 1.3% H_2 gas in the present study. However, since even 0.5% H_2 gas was shown to limit infarct size in previous work [5], 1.3% or even 1% H_2 gas may be sufficient to reduce infarct size in humans. Further, it may be a good idea to use H_2 saline because several studies have shown the cytoprotective effects of H_2 saline [4, 18, 33–38]. Second, we sometimes use carperitide, nicorandil, or nitrate upon reperfusion in patients with AMI as an adjunct therapy, and these drugs might weaken the ability of H_2 gas to limit infarct size. Carperitide and nitrate have been reported to use pathways other than mK_{ATP} [39–41]; however, nicorandil may share this pathway with H_2 gas. However, since neither nicorandil nor H_2 gas fully opens mK_{ATP} channels in vivo, the combination of these two chemicals may be additive or synergistic in limiting infarct size. Third, we observed that inhalation of H_2 gas also tended to reduce the incidence of lethal ventricular arrhythmia such as ventricular tachycardia and Vf. Although we did not precisely investigate the cellular mechanisms whereby H_2 gas limited the incidence of lethal arrhythmia, we assume that the opening of mK_{ATP} and the inhibition of mPTP may be primarily or secondarily involved (Table 2).

Although we need to overcome many issues to translate the present findings, we are encouraged to further

investigate this issue by the fact that we observed H_2 gas-induced cardioprotection in large animals and the mechanism is attributable to the activation of mK_{ATP} followed by the inhibition of mPTP.

Acknowledgements This work was supported by the Grants-in-aid from the Ministry of Health, Labor, and Welfare-Japan (H23-Nanchi-Ippan-22 to M.K.) and Grants-in-aid from the Ministry of Education, Culture, Sports, Science and Technology-Japan (21390251 to M.K.) and Grants from the Japan Heart Foundation and Grants from the Japan Cardiovascular Research Foundation. The authors thank Akiko Ogai for her technical assistance; Hatsue Ishibashi-Ueda for advice about TUNEL staining and Imai Nobuyoshi for his technical assistance with TUNEL staining; Kyoko Shioya for her assistance with animal care; Toshiyasu Asahara and Masaharu Onogi (TAIYO NIPPON SANSO Co.) for providing information about hydrogen.

Conflict of interest The authors declare that they have no conflict of interest.

References

1. Ovize M, Baxter GF, Di Lisa F, et al. Postconditioning and protection from reperfusion injury: where do we stand? Position paper from the Working Group of Cellular Biology of the Heart of the European Society of Cardiology. Cardiovasc Res. 2010;87:406–23.
2. Hausenloy DJ, Baxter G, Bell R, et al. Translating novel strategies for cardioprotection: the Hatter Workshop Recommendations. Basic Res Cardiol. 2010;105:677–86.
3. Kitakaze M, Asakura M, Kim J, et al. Human atrial natriuretic peptide and nicorandil as adjuncts to reperfusion treatment for acute myocardial infarction (J-WIND): two randomised trials. Lancet. 2007;370:1483–93.
4. Sun Q, Kang Z, Cai J, et al. Hydrogen-rich saline protects myocardium against ischemia/reperfusion injury in rats. Exp Biol Med. 2009;234:1212–9.
5. Hayashida K, Sano M, Ohsawa I, et al. Inhalation of hydrogen gas reduces infarct size in the rat model of myocardial ischemia–reperfusion injury. Biochem Biophys Res Commun. 2008;373:30–5.
6. Hausenloy DJ, Ong S-B, Yellon DM. The mitochondrial permeability transition pore as a target for preconditioning and postconditioning. Basic Res Cardiol. 2009;104:189–202.
7. Di Lisa F, Canton M, Carpi A, et al. Mitochondrial injury and protection in ischemic pre- and postconditioning. Antioxid Redox Signal. 2011;14:881–91.
8. Heusch G, Boengler K, Schulz R. Inhibition of mitochondrial permeability transition pore opening: the Holy Grail of cardioprotection. Basic Res Cardiol. 2010;105:151–4.
9. Piot C, Croisille P, Staat P, et al. Effect of cyclosporine on reperfusion injury in acute myocardial infarction. N Engl J Med. 2008;359:473–81.
10. Ohsawa I, Ishikawa M, Takahashi K, et al. Hydrogen acts as a therapeutic antioxidant by selectively reducing cytotoxic oxygen radicals. Nat Med. 2007;13:688–94.
11. Kitakaze M, Node K, Minamino T, et al. Role of activation of protein kinase C in the infarct size-limiting effect of ischemic preconditioning through activation of ecto-5′-nucleotidase. Circulation. 1996;93:781–91.
12. Mori H, Haruyama S, Shinozaki Y, et al. New nonradioactive microspheres and more sensitive X-ray fluorescence to measure regional blood flow. Am J Physiol. 1992;263:H1946–57.
13. Kitakaze M, Node K, Minamino T, et al. Role of nitric oxide in regulation of coronary blood flow during myocardial ischemia in dogs. J Am Coll Cardiol. 1996;27:1804–12.
14. Kitakaze M, Node K, Takashima S, et al. Role of cellular acidosis in production of nitric oxide in canine ischemic myocardium. J Mol Cell Cardiol. 2001;33:1727–37.
15. Kung G, Konstantinidis K, Kitsis RN. Programmed necrosis, not apoptosis, in the heart. Circ Res. 2011;108:1017–36.
16. Fukuda K-I, Asoh S, Ishikawa M, Yamamoto Y, Ohsawa I, Ohta S. Inhalation of hydrogen gas suppresses hepatic injury caused by ischemia/reperfusion through reducing oxidative stress. Biochem Biophys Res Commun. 2007;361:670–4.
17. Buchholz BM, Kaczorowski DJ, Sugimoto R, et al. Hydrogen inhalation ameliorates oxidative stress in transplantation induced intestinal graft injury. Am J Transplant. 2008;8:2015–24.
18. Cai J, Kang Z, Liu K, et al. Neuroprotective effects of hydrogen saline in neonatal hypoxia–ischemia rat model. Brain Res. 2009;1256:129–37.
19. Li J, Wang C, Zhang JH, Cai JM, Cao YP, Sun XJ. Hydrogen-rich saline improves memory function in a rat model of amyloid-beta-induced Alzheimer's disease by reduction of oxidative stress. Brain Res. 2010;1328:152–61.
20. Tsukamoto O, Asanuma H, Kim J, et al. A role of opening of mitochondrial ATP-sensitive potassium channels in the infarct size-limiting effect of ischemic preconditioning via activation of protein kinase C in the canine heart. Biochem Biophys Res Commun. 2005;338:1460–6.
21. Hanley P, Daut J. K channels and preconditioning: a re-examination of the role of mitochondrial K channels and an overview of alternative mechanisms. J Mol Cell Cardiol. 2005;39:17–50.
22. Kitakaze M, Minamino T, Node K, et al. Role of activation of ectosolic 5′-nucleotidase in the cardioprotection mediated by opening of K+c channels. Am J Physiol. 1996;270:H1744–56.
23. O'Rourke B. Myocardial K(ATP) channels in preconditioning. Circ Res. 2000;87:845–55.
24. Hausenloy DJ, Maddock HL, Baxter GF, Yellon DM. Inhibiting mitochondrial permeability transition pore opening: a new paradigm for myocardial preconditioning? Cardiovasc Res. 2002;55:534–43.
25. Lim SY, Davidson SM, Hausenloy DJ, Yellon DM. Preconditioning and postconditioning: the essential role of the mitochondrial permeability transition pore. Cardiovasc Res. 2007;75:530–5.
26. Murata M, Akao M, O'Rourke B, Marban E. Mitochondrial ATP-sensitive potassium channels attenuate matrix Ca2+ overload during simulated ischemia and reperfusion: possible mechanism of cardioprotection. Circ Res. 2001;89:891–8.
27. Hausenloy DJ. Preconditioning protects by inhibiting the mitochondrial permeability transition. AJP Heart Circ Physiol. 2004;287:H841–9.
28. Costa ADT. The mechanism by which the mitochondrial ATP-sensitive K+ channel opening and H2O2 inhibit the mitochondrial permeability transition. J Biol Chem. 2006;281:20801–8.
29. Juhaszova M, Zorov DB, Kim SH, et al. Glycogen synthase kinase-3beta mediates convergence of protection signaling to inhibit the mitochondrial permeability transition pore. J Clin Invest. 2004;113:1535–49.
30. Terashima Y, Sato T, Yano T, et al. Roles of phospho-GSK-3β in myocardial protection afforded by activation of the mitochondrial KATP channel. J Mol Cell Cardiol. 2010;49:762–70.
31. Heusch G, Boengler K, Schulz R. Cardioprotection: nitric oxide, protein kinases, and mitochondria. Circulation. 2008;118:1915–9.
32. Hammer HF. Colonic hydrogen absorption: quantification of its effect on hydrogen accumulation caused by bacterial fermentation of carbohydrates. Gut. 1993;34:818–22.

33. Chen H, Sun YP, Hu PF, et al. The effects of hydrogen-rich saline on the contractile and structural changes of intestine induced by ischemia-reperfusion in rats. J Surg Res. 2011;167:316–22.
34. Mao YF, Zheng XF, Cai JM, et al. Hydrogen-rich saline reduces lung injury induced by intestinal ischemia/reperfusion in rats. Biochem Biophys Res Commun. 2009;381:602–5.
35. Wang F, Yu G, Liu SY, et al. Hydrogen-rich saline protects against renal ischemia/reperfusion injury in rats. J Surg Res. 2011;167:e339–44.
36. Liu Q, Shen WF, Sun HY, et al. Hydrogen-rich saline protects against liver injury in rats with obstructive jaundice. Liver Int. 2010;30:958–68.
37. Chen C, Chen Q, Mao Y, et al. Hydrogen-rich saline protects against spinal cord injury in rats. Neurochem Res. 2010;35:1111–8.
38. Zheng X, Mao Y, Cai J, et al. Hydrogen-rich saline protects against intestinal ischemia/reperfusion injury in rats. Free Radic Res. 2009;43:478–84.
39. John SW, Krege JH, Oliver PM, et al. Genetic decreases in atrial natriuretic peptide and salt-sensitive hypertension. Science. 1995;267:679–81.
40. Ignarro LJ, Buga GM, Wood KS, Byrns RE, Chaudhuri G. Endothelium-derived relaxing factor produced and released from artery and vein is nitric oxide. Proc Natl Acad Sci U S A. 1987;84:9265–9.
41. Murad F. Cellular signaling with nitric oxide and cyclic GMP. Braz J Med Biol Res. 1999;32:1317–27.

Journal of Controlled Release xxx (2012) xxx–xxx

Contents lists available at SciVerse ScienceDirect

Journal of Controlled Release

journal homepage: www.elsevier.com/locate/jconrel

Amelioration of cerebral ischemia–reperfusion injury based on liposomal drug delivery system with asialo-erythropoietin

Takayuki Ishii [a,b], Tomohiro Asai [a], Dai Oyama [a], Tatsuya Fukuta [a], Nodoka Yasuda [a], Kosuke Shimizu [a], Tetsuo Minamino [c], Naoto Oku [a,*]

[a] Department of Medical Biochemistry and Global COE, School of Pharmaceutical Sciences, University of Shizuoka, 52-1 Yada, Suruga-ku, Shizuoka 422-8526, Japan
[b] Japan Society for the Promotion of Science (JSPS), 8 Ichibancho, Chiyoda-ku, Tokyo 102-8472, Japan
[c] Department of Cardiovascular Medicine, Osaka University Graduate School of Medicine, 2-2 Yamadaoka, Suita, Osaka 565-0871, Japan

ARTICLE INFO

Article history:
Received 13 December 2011
Accepted 6 February 2012
Available online xxxx

Keywords:
Ischemic stroke
Liposome
Middle cerebral artery occlusion
Nanoparticle
Neuroprotection

ABSTRACT

Cerebral ischemia–reperfusion (I/R) injury induces secondary cerebral damage. As drugs for treating this type of injury have shown poor efficacy and adverse side effects in clinical trials, a novel therapeutic strategy has been long awaited. In this study, we focused on the disruption of the blood–brain barrier after stroke, and applied a liposomal drug delivery system (DDS) designed to enhance the pharmacological effect of the neuroprotectant and to avoid side effects. PEGylated liposomes were injected at varying time after the start of reperfusion in transient middle cerebral artery occlusion (t-MCAO) model rats. The results showed PEGylated liposomes accumulated in the ischemic hemisphere at an early stage after reperfusion and were retained in the lesion for at least 24 h after injection. We also investigated the effectiveness of asialo-erythropoietin (AEPO)-modified PEGylated liposomes (AEPO-liposomes) in treating the cerebral I/R injury. AEPO-liposome treatment significantly reduced TTC-defined cerebral legion following cerebral I/R injury, and ameliorated motor function compared with vehicle and AEPO treatment. In conclusion, these results indicate that AEPO-liposomes are a promising liposomal formulation for protecting the brain from I/R injury, and that this liposomal DDS has potential as a novel strategy for the treatment of cerebral I/R injury.

1. Introduction

Cerebral vascular permeability increases after cerebral stroke, disrupting the integrity of the blood–brain barrier (BBB) via several mediators [1,2]. Although BBB disruption causes cerebral edema, resulting in neurological deficits [3], this increase in cerebral vascular permeability also permits drugs, which cannot penetrate the BBB under the normal condition, to accumulate in the brain parenchyma. A therapeutic strategy focused on increasing cerebral vascular permeability has succeeded in the treatment of some diseases [4]. Nanoparticles such as liposomes are used as a drug carrier for such a therapeutic strategy. They pass through the intercellular space between vascular endothelial cells and accumulate in the tissue owing to the enhanced permeability and retention (EPR) effect [5–9]. In addition, polyethylene glycol-modified liposomes (PEGylated liposomes) possess a long circulating property in the bloodstream by avoiding interaction with opsonins and the cells of the mononuclear phagocytic system [10]. PEGylated liposomes have been used to increase drug stability, safety, and bioavailability in humans.

Cerebral ischemia/reperfusion (I/R) injury is a secondary injury caused by oxidative stresses and inflammatory responses after recovery from cerebral ischemia [11,12], and this injury worsens the pathological condition. Although the results of many experimental and clinical studies have been published, effective therapeutic strategies for the treatment of acute stroke have not yet been achieved, due to poor efficacy and to adverse side effects in clinical trials [13–16]. Therefore, an increase in drug efficacy with fewer side effects is highly desirable for achieving neuroprotection in stroke patients.

In recent years, erythropoietin (EPO) has been shown to be cytoprotective in the brain [17,18]. Indeed, EPO binds to EPO receptor (EPOR) expressed on neuronal cells and reduces brain damage by activating MAPK and PI3K/Akt, and by increasing the expression of Bcl-x, resulting in the improvement of cerebral stroke outcome in permanent or transient cerebral ischemic animal models [18–21]. Moreover, EPOR-knockout mice show increased sensitivity to hypoxia and apoptosis of brain cells [22]. These data indicate that EPO acts as one of the important factors for neuroprotection and neurodevelopment after an ischemic event. However, multiple dosing with EPO might worsen the cerebral injury after a stroke; because the EPO-induced increase in the hematocrit may possibly induce thrombotic complications. Asialo-EPO (AEPO) is a metabolite of EPO that has no hematopoietic effect [23]. AEPO binds to the EPOR more strongly than does EPO because of the net positive charge afforded

* Corresponding author.
E-mail address: oku@u-shizuoka-ken.ac.jp (N. Oku).

0168-3659/$ – see front matter © 2012 Published by Elsevier B.V.
doi:10.1016/j.jconrel.2012.02.004

by desialylation, resulting in a strong cytoprotective effect [24,25]. Although AEPO might be expected to be an effective agent for the treatment of cerebral I/R injury, it shows low accumulation in the brain parenchyma because of its short half-life. Therefore, some method of increasing the accumulation of AEPO at the site on a cerebral injury is a potential therapeutic strategy for cerebral I/R injury.

In this study, we investigated whether a liposomal DDS could be applied as a new strategy for the treatment of cerebral I/R injury. In addition, we developed AEPO-modified PEGylated liposomes (AEPO-liposomes) as a neuroprotective agent and examined the therapeutic efficacy of AEPO-liposomes in model rats with transient cerebral ischemia.

2. Materials and methods

2.1. Animal

Male Wistar rats (170–210 g) were purchased from Japan SLC, Inc. (Shizuoka, Japan). The animals were cared for according to the Animal Facility Guidelines of the University of Shizuoka. All animal procedures were approved by the Animal and Ethics Review Committee of the University of Shizuoka.

2.2. Transient middle cerebral artery occlusion model rats

Transient middle cerebral artery occlusion (t-MCAO) model rats were prepared as described previously [26]. In brief, anesthesia was induced with 3% isoflurane and maintained with 1.5% isoflurane during cerebral stroke surgery. Rectal temperature was maintained at 37 °C with a heating pad. After a median incision of the neck skin, the right carotid artery, external carotid artery, and internal carotid artery (ICA) were isolated with careful conservation of the vagal nerve. A 4-0 monofilament nylon filament coated with silicon was introduced into the right ICA and advanced to the origin of the MCA to occlude it. Silk thread was used for ligation to keep the filament at the site of insertion into the MCA. After the operation, the neck was closed and anesthesia was discontinued. MCAO was performed for 1 h. Success of the surgery was judged by the appearance of hemiparesis. Reperfusion was performed by withdrawing the filament about 10 mm at 1 h after the occlusion under isoflurane anesthesia.

2.3. Preparation of PEGylated liposomes

PEGylated liposomes composed of distearoylphosphatidylcholine (DSPC), cholesterol, and distearoylphosphatidylethanolamine (DSPE)-PEG (M.W. of PEG was 2000) (20/10/1 as molar ratio) were prepared as follows: lipids dissolved in chloroform were evaporated to form a thin lipid film by using a rotary evaporator. The lipid film was dried for at least 1 h under reduced pressure. The dried lipid film was hydrated with PBS (pH 7.4). The liposome solution was freeze-thawed for 3 cycles with liquid nitrogen and then sonicated for 15 min at 65 °C. Finally, the particle size of liposomes was adjusted by extrusion through 100 nm-pore size polycarbonate filters (Nuclepore, Cambridge, MA, USA). For some experiments, DiI-C_{18} (Molecular Probes Inc., Eugene, OR, USA) or [^{3}H]cholesteryl hexadecyl ether (Perkin Elmer, Boston, MA) was mixed with initial lipid solution for labeling the liposomes.

2.4. Cerebral distribution of PEGylated liposomes

PEGylated liposomes were fluorescently labeled with DiI-C18. 10-mM DiI-labeled PEGylated liposomes (0.5 mL) were intravenously injected into the t-MCAO model rats at 0, 1, 3, 6 or 24 h of reperfusion. Their brains were dissected at 1 h after the injection and sliced into 2-mm thick coronal sections with a rat brain slicer (Muromachi Kikai, Tokyo, Japan). All sections were put in glass slides, and the fluorescence of DiI was measured with an *in vivo* imaging system (IVIS, Xenogen Corp., Alameda, CA).

2.5. Preparation of AEPO-liposomes

Distearoylphosphatidylethanolamine (DSPE)-PEG-*N*-hydroxysuccinimide (NHS) (0.145 mg) dissolved in 480 μL of borate buffer (pH 8.4) was mixed with 20 μL of AEPO solution (0.9 mg/mL in PBS), and the mixture was incubated for 1 day at room temperature to prepare DSPE-PEG-AEPO conjugates. A 20-mM solution of PEGylated liposomes was prepared, and then 1 mL of the liposomes was incubated with 0.5 mL of the DSPE-PEG-AEPO conjugates for 15 min at 65 °C. The AEPO-modified liposomes (AEPO-liposomes) were purified by gel filtration with Sepharose™ 4 Fast Flow (Amersham Biosciences, Sweden). The AEPO concentration of AEPO-liposomes was measured by HPLC.

2.6. Cell culture

Pheochromocytoma cells (PC12 cells, ECACC, UK) were cultured in high-glucose DME medium (WAKO, Osaka, Japan) supplemented with streptomycin (100 μg/ml), penicillin (100 units/ml), heat-inactivated 5% fetal bovine serum (FBS, Japan Bioserum, Tokyo, Japan), and 10% horse serum (HS, MP Biomedicals, Solon, OH, USA) at 37 °C in a humidified chamber with 5% CO_2.

The PC12 cells were plated on poly-D-lysine-coated 24-well plates for the MTT assay. These cells were caused to differentiate by adding nerve growth factor (NGF) at 100 ng/ml to the DME medium containing 0.5% HS at a 48-h interval. Five days after NGF treatment, these cells were used for subsequent experiments.

2.7. Cell viability assays

Differentiated PC12 cells were treated with AEPO-liposomes (0.01, 0.1 or 1.0 nmol/L as AEPO dose) or AEPO (0.1 nmol/L) for 5 days at a 48-h interval. The number of viable cells was measured by use of TetraColor™ One (Seikagaku, Tokyo, Japan). Briefly, TetraColar™ One solution was added to each well, and the cells were then incubated at 37 °C for 3 h in a humidified atmosphere containing 5% CO_2. Absorbance at 450 nm was measured by using a Tecan Infinite M200 microplate reader (Tecan, Männedorf, Switzerland)

2.8. Biodistribution of AEPO-liposomes

For determination of the biodistribution of AEPO-liposomes, AEPO was radiolabeled with ^{125}I. Briefly, IODO-BEADS® Iodination Reagent (Pierce, Rockford, IL) was added to a Na^{125}I solution (1 mCi, 890 μL), and the mixture was incubated for 5 min. AEPO solution (110 μL) was then added to the reacted solution, and incubation conducted for 15 min. For removal of excess Na^{125}I or unincorporated ^{125}I, the mixture was applied to a Zeba™ Desalt Spin Column (Pierce, Rockford, IL) and centrifuged at 1000 × *g* for 2 min.

^{125}I-labeled AEPO-liposomes were intravenously injected into the t-MCAO rats just after the start of reperfusion. At 3 and 24 h of reperfusion, the rats were sacrificed, and the blood was collected. Then the brain, heart, lung, liver, spleen, kidney, thyroid, and femur were removed and weighed. The radioactivities of organs were measured by using a gamma counter (Aloka, Tokyo, Japan).

2.9. TUNEL staining

Brains of t-MCAO model rats were dissected at 24 h after the injection of PBS or AEPO-liposomes (8 μg/kg as AEPO dose), embedded in OCT compound (Sakura Finetek, Torrance, USA), and then frozen in dry ice/ethanol. Frozen sections (10 μm) were prepared by using a cryostatic microtome (HM 505E, Microm, Walldorf, Germany) and were stained with TUNEL reagents supplied in an ApopTag® Plus Fluorescein

Please cite this article as: T. Ishii, et al., Amelioration of cerebral ischemia–reperfusion injury based on liposomal drug delivery system with asialo-erythropoietin, J. Control. Release (2012), doi:10.1016/j.jconrel.2012.02.004